Contributed Talks

(alphabetically ordered following the speaker's surname)

Hansjörg Albrecher
Reinhold Kainhofer
Robert F. Tichy
Department of Mathematics
Graz University of Technology
Steyrergasse 30/II
A-8010 Graz, Austria
e-mail: `albrecher@tugraz.at`
`http://www.cis.TUGraz.at/matha`

Title

Simulation Methods in Ruin Models
with Non-linear Dividend Barriers [1]

Abstract

In this paper we consider a collective risk reserve process of an insurance portfolio characterized by a homogeneous Poisson claim number process, a constant premium flow and independent and identically distributed claims. In the presence of a non-linear dividend barrier strategy and interest on the free reserve we derive equations for the probability of ruin and the expected present value of dividend payments which give rise to several numerical number-theoretic solution techniques. For various claim size distributions and a parabolic barrier numerical tests and comparisons of these techniques are performed.
In particular, the efficiency gain obtained by implementing low-discrepancy sequences instead of pseudorandom sequences is investigated.

112

James B. Anderson
Department of Chemistry
Pennsylvania State University
University Park, Pennsylvania 16802
e-mail: jba@psu.edu
http://random.chem.psu.edu

TITLE

Quantum Monte Carlo:
Direct Calculation of Corrections to Trial Wave Functions and Their Energies

ABSTRACT

We will discuss an improved Monte Carlo method for calculating the difference δ between a true wavefunction Ψ and an analytic trial wavefunction Ψ_0. The method also produces a correction to the expectation value of the energy for the trial function. Applications to several sample problems as well as to the water molecule will be described.

We have described previously a quantum Monte Carlo (QMC) method for the direct calculation of corrections to trial wavefunctions [1-3]. Our improved method is much simpler to use. Like its predecessors the improved method gives (for fixed nodes) the difference δ between a true wavefunction Ψ and a trial wavefunction Ψ_0, but it gives in addition the difference between the true energy E and the expectation value of the energy E_{var} for the trial wavefunction.

The statistical or sampling errors associated with the Monte Carlo procedures as well as any systematic errors occur only in the corrections. Thus, very accurate wavefunctions and energies may be corrected with very simple calculations.

For systems with nodes the nodes are unchanged. The wavefunctions and energies for these systems are corrected to the fixed-node values - those corresponding to the exact solutions for the fixed nodes of the trial wavefunctions.

The method has the very desirable features of: good wavefunction in / better wavefunction out ... good energy in / better energy out.

The ground state of the helium atom provides a simple example. We used as a trial wavefunction the 189-term Hylleraas function described by Schwartz [4] which is accurate to about 10 digits. The true energy is known to at least 13 digits from the analytic variational calculation of Freund, Huxtable, and Morgan [5] with a more complex trial function.

The expectation value for the trial function is $-2.903\,724\,376\,180(0)$ hartrees. The calculated correction is $-0.000\,000\,000\,856(2)$ hartrees which gives a corrected value of $-2.903\,724\,377\,036(2)$ hartrees. This may be compared with the known value of $-2.903\,724\,377\,034(0)$ hartrees.

The water molecule presents the problem of nodes in the wavefunction as well as a much higher dimensionality. In this case the nodes are fixed in position by the use of fixed-node QMC procedures [6] and the resulting energy obtained is the fixed-node energy for the nodes of the trial wavefunction. As in any fixed-node calculation the energy obtained is a variational

upper bound to the true energy, and if the nodes are wrong the energy will be higher than the true energy.

The trial function for this case was a simple SCF function, consisting of a single 10x10 determinant of LCAO-MO terms of Slater-type orbitals without any Jastrow or other explicit electron correlation terms. The expectation value of the energy for the trial function and the fixed-node QMC energy were determined independently by standard methods.

In this case the initial energy is -75.560 hartrees, the calculated correction is -0.599 hartrees, and the corrected value is $-76.169(10)$ hartrees. This may be compared with the independently calculated value of $-76.170(10)$ hartrees.

Earlier fixed-node QMC calculations for systems of ten or more electrons have used single-determinant trial wavefunctions with Jastrow terms. With the improved correction procedure the need for accurate expectation values for the trial function requires eliminating the Jastrow terms, but it may make practical the use of many more determinants in the trial function. This is likely to give improved node locations and lead to much lower node location errors. The sign problem of quantum Monte Carlo for large systems would not be eliminated but it might be significantly reduced.

[1] J. B. Anderson and B. H. Freihaut, J. Comput. Phys. **31**, 425 (1979).

[2] J. B. Anderson, J. Chem. Phys. **73**, 3897 (1980).

[3] J. B. Anderson, M. Mella, and A. Luechow, in Recent Advances in Quantum Monte Carlo Methods, (W. A. Lester, Jr., Ed., World Scientific, Singapore) 1997, pp. 21-38.

[4] C. Schwartz, Phys. Rev. **128**, 1146 (1962).

[5] D. E. Freund, B. D. Huxtable, and J. D. Morgan III, Phys. Rev. A **29**, 980 (1984).

[6] J. B. Anderson, J. Chem. Phys. **63**, 1499 (1975).

James B. Anderson[1]
Lyle N. Long[2]
[1]Department of Chemistry
[2]Department of Aerospace Engineering
Pennsylvania State University
University Park, Pennsylvania 16802
e-mail: `jba@psu.edu`
`http://random.chem.psu.edu`

TITLE

The Simulation of Detonations

ABSTRACT

The Direct Simulation Monte Carlo (DSMC) method (1,2) has been found remarkably successful for predicting and understanding a number of difficult problems in rarefied gas dynamics. Extension to chemical reaction systems has provided a very powerful tool for reacting gas mixtures with non-Maxwellian velocity distributions, with non-Boltzmann state distributions, with coupled gas-dynamic and reaction effects, with concentration gradients, and with many other effects difficult or impossible to treat in any other way. Examples of systems which may be treated include flames and explosions, shock waves and detonations, reactions and energy transfer in laser cavities, upper atmosphere reactions, and many, many others. In this paper we will discuss the application of the DSMC method to the problem of detonations, a classic and extreme example of the coupling of gas dynamics and chemical kinetics.

Although a Monte Carlo simulation of a gas was described by Lord Kelvin in 1901 (3), it was not until the 1960's that the use of such simulations became practical for solving problems in the field of rarefied gas dynamics. The combination of an efficient sampling method by Bird (1) in 1963 with high speed computers made possible the nearly exact simulation of a number of systems that had earlier been impossible to analyze. The current generation of computers makes it possible to consider much more ambitious applications: those in which chemical reactions are important.

A detonation wave travels at supersonic speed in a reactive gas mixture and is driven by the energy released in exothermic reaction within the wave. The modern theory of detonations begins with the work of Chapman and of Jouguet about 1900, and their work has been extended by a number of others, in particular by Zeldovich (4), von Neumann (5), and Döring (6). These three arrived independently at an expression, the ZVD expression, giving the velocity of a detonation wave as the velocity of sound in the completely burned gases when the shock wave precedes the reaction.

In order to simplify our DSMC calculations and to clarify the results by eliminating extraneous effects, we considered the special case of the reaction of $A + M \rightarrow B + M$ in which the masses of A, B, and M are equal. The gases were specified as ideal and calorically perfect with constant heat capacities. The cross-sections for reaction were specified as simple functions of collision energy corresponding to Arrhenius behavior. Calculations were carried out for a variety of conditions - covering a wide range of exothermicities and reaction rate parameters.

The simulations provide complete details of the properties of the system as they vary across the detonation wave. A variety of interesting results have been obtained. Temperature, density, and reaction-rate peaks may be separated. Temperature and density maxima depend strongly on reaction rate. The thickness of the reaction zone depends strongly on conditions. The results provide severe tests for some of the earlier theoretical models of detonations.

(1) G. A. Bird, Phys. Fluids **6**, 1518 (1963).

(2) G. A. Bird, Molecular Gas Dynamics and the Direct Simulation of Gas flows, Clarendon Press, Oxford, 1994.

(3) Lord Kelvin, Phil. Mag. (London) **2**, 1 (1901).

(4) Y. B. Zeldovich, J. Exptl. Theoret. Phys. (U.S.S.R.) **10**, 542 (1940).

(5) J. von Neumann, O.S.R.D. Rept. No. 549 (1942).

(6) W. Döring, Ann. Physik **43**, 421 (1943).

James B. Anderson
Department of Chemistry
Pennsylvania State University
University Park, Pennsylvania 16802
e-mail: `jba@psu.edu`
`http://random.chem.psu.edu`

Title

Monte Carlo Treatment of UV Light Imprisonment in Fluorescent Lamps

Abstract

The efficiency of a modern fluorescent lamp is reduced significantly by self-absorption of the 2537-Å ultraviolet radiation emitted from mercury within the lamp (1). Experimental measurements indicate the efficiency may be increased by tailoring the isotopic composition of the mercury as by the addition of $^{196}_{80}$Hg to natural mercury (2).

Radiation emitted by an atom in an optical transition from an excited state to the ground state is commonly called "resonance radiation." Since the cross-section for absorption of this radiation by atoms in the ground state is typically large, a quantum of radiation released within a chamber containing emitting atoms is likely to be reabsorbed before reaching the walls of the chamber. The absorbing atom may subsequently emit the radiation, and the emission-absorption steps may be repeated a large number of times. The radiation is described as "imprisoned" or "trapped" when the number of steps required for escape to the walls is large.

The imprisonment of resonance radiation in the electrical discharge of fluorescent lamps can be treated by Monte Carlo methods. The calculation of radiation and energy transfer is essentially a simulation of the processes occurring within the lamp. Following the initial excitation of a mercury atom its energy (or photon) is tracked from atom to atom until the photon either leaves the system or is lost by quenching in the collision of an excited atom with another atom. The procedure is repeated thousands of times to obtain a reliable estimate of the overall exit probability and a spectrum of the exit radiation with an acceptable noise level.

Many of the variables required in the calculation are selected from appropriately weighted distributions. For example, an initial isotopic species to be excited is selected with a probability proportional to its fraction in the mixture. The direction of an emitted photon is selected at random in three dimensions. The frequency of the emitted radiation is selected from a Voigt distribution with the line center corresponding to that of the excited atom. The free path of a photon is selected from the calculated distribution of free paths for a photon with the same wavelength.

The effects of emission and absorption linewidths, hyperfine splitting, isotopic composition, collisional transfers of excitation, and quenching are explicitly included in the calculations. The calculated spectra of the emitted radiation are in good agreement with measured spectra for several combinations of lamp temperature and mercury composition. The complete details

of the hyperfine structure of the spectra including multiple peaks for the isotopes and line-reversal are accurately reproduced. Also in agreement with experiments, the addition of $^{196}_{80}$Hg to natural mercury is found to increase lamp efficiency.

(1) J. F. Waymouth, "Physics for Fun and Profit", Physics Today **54**, 38 (2001).

(2) J. Maya, M. W. Grossman, R. Laguschenko, and J. F. Waymouth, Science **226**, 435 (1984).

F. M. Bufler[1]
A. Schenk
W. Fichtner
Institut für Integrierte Systeme
ETH Zürich
Gloriastrasse 35
CH-8092 Zürich, Switzerland
e-mail: `bufler@iis.ee.ethz.ch`
`http://www.iis.ee.ethz.ch/portrait/staff/bufler.en.html`

TITLE

Proof of a Simple Time–Step Propagation Scheme
for Monte Carlo Simulation[2]

ABSTRACT

Monte Carlo simulation has been established as a stochastic method for the solution of the Boltzmann transport equation (BE) (1; 2; 3) which is an integro–differential equation for the electron distribution function. Its solution can be used to compute macroscopic quantities such as the electron density or the current density. Since the BE considers the electron drift in the electric field as well as the scattering events at a microscopic level, it allows one to take physical effects occurring in deep submicron metal–oxide–semiconductor field–effect transistors (MOSFETs) into account, for example ballistic and hot–electron transport. Various algorithms have been developed to improve the computational efficiency of the Monte Carlo simulation. Among them is the self–scattering scheme of Rees (4) which uses an upper estimate Γ of the scattering rate to greatly facilitate the determination of the collisionless flight–time. In order to avoid at the same time a large number of self–scattering events involved with a global upper estimation, a variable Γ scheme is often being employed (1; 5; 6; 7). This scheme is especially useful for full–band Monte Carlo (FBMC) simulation where the electronic band structure is not described by an analytical formula, but computed by the empirical pseudopotential method and stored in a table. Here it is natural to assign a different Γ to each element of the discretized phase–space. However, for large selected free–flight times the electron will leave the original phase–space element and the flight–time is usually adjusted in a rather complicated manner in order to accomodate the change of Γ (5; 6; 7). It is the aim of this paper to show that such an adjustment is not necessary, but that simply a new flight–time can be stochastically selected if the border of the original phase–space element is crossed.

The proof is based on the calculation of the probability that there is no scattering between the times 0 and t. This event is equivalent to the time of the first scattering, t_s, being larger than t and therefore the event will be denoted by $\{t_s \notin (0, t)\}$. When the time interval $(0, t)$ is decomposed into two not necessarily equidistant time intervals, the above event can be represented as the intersection of the events that there is no scattering in any of the two intervals, i.e. we have for the corresponding probability

---

$$P(\{t_s \notin (0,t)\}) = P(\{t_s \notin (0,t_1)\} \cap \{t_s \notin (t_1,t)\}) \tag{1}$$

Equation (1) is completely general and does not refer to the Boltzmann transport equation (BE). On the other hand, in the specific case of the BE, this probability is given by (8; 9)

$$P_{\text{BE}}(\{t_s \notin (0,t)\}) = \exp\left(-\int_0^t S(\mathbf{k}(\tau))\,d\tau\right) \tag{2}$$

where S is the scattering rate and $\mathbf{k}(\tau)$ the electron's momentum at time τ. The exponential in Eq. (2) allows a factorization according to

$$
\begin{aligned}
P_{\text{BE}}(\{t_s \notin (0,t)\}) &= P_{\text{BE}}(\{t_s \notin (0,t_1)\} \cap \{t_s \notin (t_1,t)\}) \\
&= \exp\left(-\left\{\int_0^{t_1} S(\mathbf{k}(\tau))\,d\tau + \int_{t_1}^t S(\mathbf{k}(\tau))\,d\tau\right\}\right) \\
&= \exp\left(-\int_0^{t_1} S(\mathbf{k}(\tau))\,d\tau\right) \times \exp\left(-\int_{t_1}^t S(\mathbf{k}(\tau))\,d\tau\right) \\
&= P_{\text{BE}}(\{t_s \notin (0,t_1)\}) \times P_{\text{BE}}(\{t_s \notin (t_1,t)\}).
\end{aligned}
\tag{3}
$$

Since $P(A \cap B) = P(A) \times P(B)$ for stochastically independent events A and B, Eq. (3) proves that the absence of scattering in the interval (t_1, t) is independent of the absence of scattering in the interval $(0, t_1)$. In other words, when the event that the first scattering does not occur before t_1 is realized (with the help of a random number r evenly distributed in $[0, 1)$), the particle can be propagated until t_1 and then a new random number can be generated to decide whether scattering occurs in the next interval.

For an explicit treatment of the opposite event, we observe regardless of the above considerations that Eq. (2) shows for $t \to \infty$ that there will occur, at some time, the first scattering. It follows that

$$P_{\text{BE}}(\{t_s \in (0,t_1)\}) = 1 - P_{\text{BE}}(\{t_s \notin (0,t_1)\}) = 1 - \exp\left(-\int_0^{t_1} S(\mathbf{k}(\tau))\,d\tau\right). \tag{4}$$

Hence, in the self–scattering scheme with an upper estimation Γ of $S(\mathbf{k})$, the event of the first scattering occurring before t_1 is realized for $r < 1 - \exp(-\Gamma t_1)$. In this case the particle is propagated as usual until $t_s = -\frac{1}{\Gamma}\ln(1-r)$. In fact, the above inequality leads to $-\ln(1-r) < \Gamma t_1$ and therefore to $t_s < t_1$.

In summary, the above considerations have proven the following propagation scheme. First, a random number is used to determine whether the first scattering occurs before a given time t_1. In this case, the particle is propagated according to the corresponding free–flight time, otherwise until t_1. Then a new, possibly different time step is defined and the procedure is repeated. The validity of this scheme has been verified by an explicit comparison with the standard Monte Carlo scheme and was used for an efficient FBMC device simulation (10).

References

[1] C. Jacoboni and P. Lugli, *The Monte Carlo Method for Semiconductor Device Simulation* (Springer, Wien, 1989).

[2] *Monte Carlo Device Simulation: Full Band and Beyond*, edited by K. Hess (Kluwer, Boston, 1991).

[3] M. V. Fischetti and S. E. Laux, Phys. Rev. B **38**, 9721 (1988).

[4] H. D. Rees, Phys. Lett. A **26**, 416 (1968).

[5] J. Bude and R. K. Smith, Semicond. Sci. Technol. **9**, 840 (1994).

[6] E. Sangiorgi, B. Ricco, and F. Venturi, IEEE Trans. Computer–Aided Des. **7**, 259 (1988).

[7] C. Jungemann, S. Keith, M. Bartels, and B. Meinerzhagen, IEICE Trans. Electron. **E82–C**, 870 (1999).

[8] W. Fawcett, A. D. Boardman, and S. Swain, J. Phys. Chem. Solids **31**, 1963 (1970).

[9] A. Reklaitis, Phys. Lett. A **88**, 367 (1982).

[10] F. M. Bufler, A. Schenk, and W. Fichtner, IEEE Trans. Electron Devices **47**, 1891 (2000).

Ervin Dubaric[1][2]
Urban Englund
Mats Hjelm[2]
Hans-Erik Nilsson
Department of Information Technology and Media
Mid-Sweden University
SE-851 70 Sundsvall, Sweden

Title

Monte Carlo Simulation of the Transient Response of Single Photon Absorption in X-ray Pixel Detectors

Abstract

A Monte Carlo method to simulate the transient response of X-ray pixel detectors is proposed. The method combines the use of a state of the art photon transport and absorption model with full band Monte Carlo simulation of the semiconductor detector. The method has been used to study the transient response of a single photon absorption event in three different X-ray pixel detectors, one photon counting detector, one integrating detector and one scintillator coated integrating pixel detector. In a photon counting detector each absorbed photon is detected as a current pulse, which in turn triggers a digital counter. In an integrating version, the current is integrated by a charge sensitive amplifier, producing an analog signal as the detector output. Coating an integrating detector with a scintillating layer increases the number of photons that can be detected by the detector. In this case the signal is generated both by X-ray photons captured in the scintillator and by X-ray photons captured directly in the semiconductor. There are different reasons to study the single photon absorption in these detector structures. In the photon counting configuration the actual output signal is the transient response of a single photon absorption event. On the other hand, in the integrating configuration the single photon event may be used to study charge sharing effects introduced by absorption in the boundary region of the pixel detector. In this case the interest is primarily to track the generated carriers as they are distributed among the neighboring pixels.

Introduction to X-ray imaging detectors

An X-ray detector can either be made from a heavy semiconductor with high stopping power for X-rays or a scintillator can be used to convert the X-ray photons to visible light, which is then sensed by a pixel sensor. In a single layer detector, made from a heavy semiconductor, the response of the system is only determined by the properties of the semiconductor. In a detector system where a scintillator and photo-detector form a two-layer system the response of the system depends both on the properties of the scintillator and the properties of the photo-detector.

---

[1]Speaker; e-mail: `Ervin.Dubaric@ite.mh.se`
[2]also: Solid State Electronics, Department of Microelectronics and Information Technology, Royal Institute of Technology (KTH), Electrum 229, SE-164 40 Kista, Sweden

In a scintillator coated X-ray imaging sensor the signal is generated both by X-ray photons captured in the scintillator and by X-ray photons captured in the semiconductor sensor. Since the amount of generated charge in the semiconductor, per MeV of absorbed X-ray energy, differs significantly depending on where the absorption occurred, the image properties are affected both by the scintillator and the semiconductor sensor.

In a photon counting system a pure semiconductor detector is used. The detector should have high charge collection efficiency, which demands the use of a very pure semiconductor material in order to obtained the highest possible $\mu \cdot \tau$ product. A typical sensor consists of a shallow PN junction, with as large depletion region in the bulk as possible.

Simulation

A method to simulate these types of detectors is proposed. The method is based on the use of two different Monte Carlo simulation software packages. The photon transport is simulated using the commercially available MCNP software and the charge carrier transport is simulated using our own full band Monte Carlo device simulator. A third, in house software, is used as a link between the two Monte Carlo simulators when simulating the scintillator coated detector. This in house software calculates the distribution and absorption of visible light in the semiconductor resulting from an X-ray absorption in the scintillating layer. A large part of this light is absorbed near the surface of the nearest pixel detector. However, depending on the design of the scintillating layer charge sharing may occur as the light is scattered towards neighboring pixels.

The simulation procedure starts by simulating the detector structure in MCNP. MCNP calculates the trajectory of incoming X-ray photons using a Monte Carlo approach. The trajectories of the simulated photons are investigated and a number of particularly interesting trajectories is selected. Each of these trajectories (including data for deposited charge along the path) is used as input in the full band Monte Carlo device simulator. In the case of an absorption in the scintillator layer, the in house light scattering program is used to transfer the signal down to the semiconductor detector. The response of the detector is then simulated using the full band Monte Carlo device simulator.

There are several important issues that need to be addressed in simulation of the detector response. The detector structures are usually very large which makes self-consistent simulation very time consuming. In this work we have used self-consistent simulations in the photon counting detector where the absorption event occurs in the depletion region. In this way we may directly record the current pulse at the detector electrodes. In the case of the integrating detectors we are following the carriers as they move towards collection. The charge sharing is studied by comparing the number of carriers absorbed at different pixel locations. The actual current pulse is not recorded, which allows us to use a constant potential profile during the simulation. The potential profile has been obtained from drift-diffusion simulation of a dark detector.

Simulation result of different detector structures is presented using this new approach. The result has primarily been used to visualize the charge sharing in pixel arrays and to study the transient response as a function of position of the absorption in photon counting detectors.

Lucian Shifren
David K. Ferry [1]
Department of Electrical Engineering
Center for Solid State Electronics Research
Arizona State University
Tempe, Arizona, 85287-5706, USA
e-mail: `ferry@asu.edu`
`http://www.eas.asu.edu/~nano`

Title

A Particle Monte Carlo Simulation
Based on the Wigner Function Distribution

Abstract

We present results of a new particle-based ensemble Monte Carlo (EMC) simulation of the Wigner distribution function (WDF). EMC of quantum systems is difficult to implement due to the particle nature of the method and the wave-like nature of the quantum phenomena. We introduced a new property for the particles, which we call the particle affinity, which allows the overall distribution to assume negative and partial electron values. We divide the simulation into two system, the first being the EMC regime, and the second being the WDF regime. Although two systems exists, the two systems work simultaneously within the simulation. Within the EMC regime, all particles in the system are treated equally, that is, all particles have an assigned position and momentum, all particles drift and are accelerated and scattered. In the WDF regime however, along with the pre-mentioned properties assigned to the electrons, we also assign the electrons an affinity. The affinity value the electron may take must have a magnitude less then one, where a value of one corresponds to a "present" electron, a value of minus one corresponds to a "minus presence," and any value in between accounts for the partial "presence" or "minus presence" of an electron. Within the simulation, all particles drift and are accelerated, independent of what their affinities might be. However, when calculating the Wigner potential (which is a non-local potential), we switch to the WDF regime. Here, the Wigner distribution is defined by

$$f\left(x, k\right) = \sum_i \delta(x - x_i)\delta(k - k_i)A\left(i\right),\tag{1}$$

where the delta functions represent the presence of a particle from the EMC regime, and A, the affinity, represents the value of the electron which is contributed to the distribution. Results using this method are shown in Fig 1. The results show a gaussian wave packet which has tunneled through a potential barrier. This result has been compared to two fully quantum mechanical simulations, namely, a full solution of Schrödinger equations and the direct solution of the WDF. The transmission coefficients of all three cases is ~ 0.35, which corresponds to the analytical value determined from simple tunneling theory. The new EMC

---

[1]Speaker; Research supported by the Office of Naval Research

method has also been checked against the other methods using Bohm trajectories which show remarkable similarity to each other. The EMC method correctly shows that the Bohm trajectories originating from the front of the gaussian packet are the ones that tunnel. Not only does the particle solution calculate the correct transmission and give the correct Bohm trajectories, but also, the resulting density displays interference effects and correlations, seen in Fig 1, that have previously only been seen in fully quantum mechanical simulations. Correlations are fully quantum mechanical and allow for time reversal in quantum systems. We believe this to be the first particle-based simulation that correctly accounts for interference, correlation and tunneling.

Figure 1: Distribution function from EMC solution of a gaussian which has tunneled through a potential barrier 2nm wide and 0.3 eV high.

S.M. Ramey
D.K. Ferry [1]
Department of Electrical Engineering and
Center for Solid State Electronics Research
Arizona State University
Tempe, Arizona, 85287-5706
USA
e-mail: `ferry@asu.edu`
`http://www.eas.asu.edu/~nano`

TITLE

Monte Carlo Modeling of Quantum Effects in Semiconductor Devices with Effective Potentials

ABSTRACT

As modern devices continue to scale to smaller sizes, it has become imperative to include quantum mechanical effects when modeling device behavior. We have recently proposed the use of the effective potential to treat the quantum mechanical effects of confinement in the region adjacent to the oxide interface [1]. In this work, we illustrate the use of the effective potential as a fast and simple method of including these effects in Monte Carlo simulation of ultrasmall SOI MOSFETs.

The effective potential concept uses the fact that as the electron moves, the edge of the wave packet encounters variations in the potential profile before the center of the wave packet. Mathematically, this effect at a point (x_i, y_j) can be treated as the convolution of the potential with the Gaussian wave packet as follows:

$$V_{eff}(x_i, y_j) = \iint V(x, y) G(x, y; x_i, y_i; a_x, a_y) dx dy$$

where G is the Gaussian function with standard deviations a_x and a_y. The spread of the wave packet is determined by the thermal de Broglie wavelength for the lateral direction and the confining potential in the transverse direction [2,3].

The effective potential is included in the Monte Carlo transport simulation by applying the above convolution to the potential found from solution of the Poisson equation. As an example, the resulting effective potential profile for an SOI NMOSFET with a 30 nm silicon layer is illustrated in Fig. 1 for an applied gate and drain voltage of 1.2 volts. The potential clearly increases at the oxide interfaces as a result of the convolution with the electron wave packet. As a result of this potential increase, the electrons experience a strong electric field, which is then included in the Monte Carlo transport kernel.

As a demonstration of this, Fig. 2 shows the electron density distribution that corresponds to the potential profile in Fig. 1. The average electron density set-back from the gate interface is about 2.5 nm, which is consistent with results shown elsewhere [3].

Figure 1: Potential profile for a 30 nm SOI NMOSFET.

Figure 2: Source and channel electron density distribution for the potential shown in Figure 1. Note: to bring out the details of the channel distribution, the drain region is not shown.

In this work we show how the charge set-back and ground state energy rise results in the expected increase in threshold voltage and reduces the drive current. The threshold voltage for the shown device increases approximately 0.2 volts when the quantum effects are included with the effective potential.

References

[1] D. K. Ferry, R. Akis, and D. Vasileska, *IEDM Conf. Rec. (IEEE Press, New York)*, 287 (2000).

[2] D.K. Ferry, *Superlatt. Microstruct.*, v.27, 61 (2000).

[3] D.K. Ferry, *VLSI Design* in press (2001).

Mary E. Flahive
Department of Mathematics
Oregon State University
Corvallis, OR U.S.A.
e-mail: `flahive@math.orst.edu`

Figure of Merit for Digital Nets over $\mathbf{Z}_2$

ABSTRACT

In this talk we will generalize some techniques from real diophantine approximation which might be helpful for locating good candidates for binary digital nets in higher dimensions. Articles (6; 8) are rich sources for the current status of digital nets over a general field and a wealth of computational information.

As Harald Niederreiter explained in Section 4.4 of (4), the theory of continued fractions can be used to identify good two-dimensional digital nets over finite fields. In Theorem A of (1), G. Larcher, A. Lauss, H. Neiderreiter, and W. Ch. Schmid further analyze this construction of nets, a construction which is reminiscent of Hlawka's good lattice points. For fixed $f \in \mathbf{Z}_2[x]$ with $\deg(f) = n \geq 2$, we set $R = \mathbf{Z}_2[x]/(f)$ and choose the coset representative of minimal degree. For any fixed dimension $s \geq 2$, the digital (t, n, s)-nets formed using $f \in \mathbf{Z}_2[x]$, $\mathbf{g} \in R^s$ have small $t = n - \rho(\mathbf{g}, f)$, where

$$\rho(\mathbf{g}, f) = s - 1 + \min\{\sum_{i=1}^{s} d(h_i) \ : \mathbf{h} \in V(\mathbf{g})\},$$

$V(\mathbf{g}) = \{\mathbf{h} \in R^s \ : \ h_1 g_1 + \ldots + h_s g_s = 0\}$, and d is defined on R by $d(0) = -1$ and $d(g) = \deg(g)$ for nonzero g.

For fixed $s \geq 2$, we would like to determine $f \in \mathbf{Z}_2[x]$ for which there exists $\mathbf{g} \in R^s$ such that $\rho(\mathbf{g}, f)$ is large and also to identify such $\mathbf{g} \in R^s$. We restrict attention to $\mathbf{g}$ whose coordinates are relatively prime to f; that is, $g_i \in U(R)$, the group of units. We then may standardize to $\mathbf{g} = (1, g_1, g_1 g_2, \ldots, g_1 \cdot g_{s-1})$. For fixed f we set $\mu(\mathbf{g}) = \rho(\mathbf{g}, f) - (s - 1)$.

As for the reals, for any $g \in U(R)$ a continued fraction can be obtained for $\frac{g}{f}$ by applying the Euclidean Algorithm to g and f as elements of $\mathbf{Z}_2[x]$. This yields the partial quotients $a_1, \ldots, a_N \in \mathbf{Z}_2[x]$ of the continued fraction for $\frac{g}{f}$. Its sequence of convergents, $\frac{p_i}{q_i}$, is obtained from using the recurrence

$$p_0 = 0, \ p_1 = 1, \ p_i = a_i p_{i-1} + p_{i-2} \ ; \ q_0 = 1, \ q_1 = a_1, \ q_i = a_i q_{i-1} + q_{i-2} \ ,$$

where $q_N = f$ and all other p_i, q_i are polynomials whose degree is less than n.

For $s = 2$: From Theorem 4.46 in (4) we obtain $\mu((1, g), f) = n - A(g)$ where $A(g) = \max\{d(a_i) \ : \ i = 1, \ldots, N\}$. With this result, the question of maximizing the two-dimensional figure of merit reduces to identifying f for which there exist $g \in U(R)$ such that $A(g) = 1$ (which we call poorly approximable g). When f has t distinct nonlinear irreducible factors

in $\mathbf{Z}_2[x]$, Jill Mesirov and Melvin Sweet prove in (3) that there exist either no or 2^t poorly approximable g, and that irreducible f always have two. Jill Lombaer, a Master of Arts student, has tabulated some poorly approximable g when $\deg(f)$ is small.

In order to obtain f which have a good figure of merit in higher dimensions, some "simultaneous approximation" of $g_1, g_2, \ldots, g_{s-1}$ in R must be excluded. For this, it seems necessary to refine our knowledge of the quality of approximation inherent in the continued fraction process. We explain this more in what follows.

Some basic observations are:

1. If $a_1, \ldots, a_N$ are the partial quotients for $g \in U(R)$ then $a_N, \ldots, a_1$ (in order) are the partial quotients for g^{-1}. From this we obtain $a_1, \ldots, a_N$ is symmetric if and only if $g^2 = 1$, which cannot hold when f is irreducible in $\mathbf{Z}_2[x]$.

2. Suppose $g^2 \neq 1$. If $\frac{p_i}{q_i}$ and $\frac{P_i}{Q_i}$ are the sequences of convergents for $\frac{g}{f}$ and $\frac{g^{-1}}{f}$, respectively, then for all $i = 0, 1, \ldots, N-1$

$$q_i g = Q_{N-i-1} \ ; Q_i g^{-1} = q_{N-i-1}.$$

3. (Analogue of Ostrowski's expansion (5; 7)) Let V denote the set of polynomials of degree less than n, considered as a vector space over $\mathbf{Z}_2$. For $d_i = d(a_i) - 1$, the sequence $f_0, \ldots, f_n$ defined by

$$q_0, q_1, xq_1, \ldots, x^{d_1} q_1, q_2, \ldots, x^{d_{N-1}} q_{N-1}$$

is a basis for V. Moreover, if the expansion of $c \in R$ is

$$c = f_{i_1} + \sum_{i_1 < i < i_s} \beta_i f_i + f_{i_s} \text{ for } i_1 \leq i_s; \beta_i \in \mathbf{Z}_2$$

then

(a) for $i_1 = d(q_k)$,

$$d(cg) = d(Q_{N-1-k}) = d(a_N) + \ldots + d(a_{N-k});$$

(b) for i_1 with $d(q_{k-1}) < i_1 < d(q_k)$,

$$d(cg) = d(x^m Q_{N-1-k}) = m + d(Q_{N-1-k}),$$

where $m = \max\{i \ : \beta_i \neq 0 \text{ and } d(q_{k-1}) < i < d(q_k) \}$.

Our object is to apply this to the three-dimensional case. The results I have right now are quite technical, but I'll try to give a general flavor: We note that

$$\mu(1, g_1, g_1 g_2) \leq \min\{\mu(1, g_1) - 1, \mu(1, g_2) - 1, \mu(1, g_1 g_2) - 1\}.$$

129

For this talk we restrict to f for which there exist $g_1 \neq g_2^{-1}$ with $A(g_1) = A(g_2) = 1$ and $A(g_1 g_2) \leq 2$. (For irreducible f this forces $g_2 = g_1$ and $A(g_1^2) = 2$.) Using the basis $\{(g_1, 1, 0), (0, 1, g_2^{-1})\}$ for $V(\mathbf{g})$, we investigate

$$\min\{d(c_1 g_1) + d(c_1 + c_2) + d(c_2 g_2^{-1}) \; : \; c_i \in R, \text{ not both zero }\}.$$

Considering $c_1, c_2 \in R$ with

$$d(c_1 g_1) + d(c_1 + c_2) + d(c_2 g_2^{-1}) \leq n - 3,$$

it follows that $d(c_1) = d(c_2) > \frac{n+1}{2}$. Labelling the convergents corresponding to g_1 and g_2^{-1} by $\{\frac{p_i}{q_i}\}$ and $\{\frac{r_i}{s_i}\}$, respectively, possible candidates are $c_1 = q_d$, $c_2 = s_d$ for $d > \frac{n+1}{2}$. Using the continued fraction process, we've shown that $d(q_d + s_d)$ cannot be "very small"; our results are not very tight. More computation will give a better idea of the fruitfulness of this approach for identifying f with good three-dimensional digital nets over $\mathbf{Z}_2$.

References

[1] G. Larcher, A. Lauss, H. Niederreiter, and W. Ch. Schmid, *Optimal polynomials for (t, m, s)-nets and numerical integration of multivariate Walsh series* Siam Journal of Numerical Analysis, **33** (1996), 2239–2253.

[2] Alain Lasjaunias, *Continued fractions for algebraic formal power series over a finite base field,* Finite Fields and their applications, **5** (1999), 46–56.

[3] Jill P. Mesirov and Melvin M. Sweet, *Continued fraction expansions of rational expressions with irreducible denominators in characteristic 2,* Journal of Number Theory, **27** (1987), 144–148.

[4] Harald Niederreiter, *Random Number Generation and Quasi-Monte Carlo Methods*, (1992) SIAM.

[5] Alexander Ostrowski, *Bemerkungen zur Theorie der Diophantischen Approximationen,* Abh. Math. Sem. Hamburg. Univ. **1** (1923), 77–98.

[6] Gottlieb Pirsic and Wolfgang Ch. Schmid, *Calculation of the Quality Parameter of Digital Nets and Application to their Construction,* preprint.

[7] Andrew M. Rockett and Peter Szusz, *Continued Fractions,* (1992) World Scientific Publishing.

[8] Wolfgang Ch. Schmid, *Improvements and extensions of the "Salzburg Tables" by using irreducible polynomials,* in Monte Carlo and Quasi-Monte Carlo Methods 1998, (1999), Springer, 436–447.

Mats Hjelm[1] [2]
Hans-Erik Nilsson
Department of Information Technology and Media
Mid-Sweden University
SE-851 70 Sundsvall, Sweden

Title

A Full Band Monte Carlo Simulator for Cubic and Hexagonal Semiconductor Materials and Devices: an Object-Oriented Approach

Abstract

A full band MC simulator consists of a number of interdependent physical models, which can be implemented using different levels of approximations. The approximation needed for each model is dependent on the application for the simulator. In an advanced device simulator, the complexity of the models needed may vary over different regions in the device. For example, in a region with few carriers a very CPU-time demanding model may be required, which may be impossible to apply in a region with higher carrier density. Processes like impact ionization, as well as injection and absorption of carriers at contacts, are best handled using dynamic memory structures. In addition, statistical enhancements in rare regions are often needed in simulations of devices with high variation of carrier concentration. These enhancements are usually achieved by letting the weight and the number of superparticles (cluster of carriers) vary in time and space during the simulation. All these different constraints make it difficult to develop a general MC device simulator. This statement is underlined by the fact that there is no such simulator available on the commercial market, although the MC method for semiconductor simulations has been known for over 20 years. Our ambition in this work is to present a thorough analysis of the requirements of a general MC device simulator. We also present how these constraints have guided the development of an MC simulator at Mid-Sweden University. Finally, we present some device simulation results for cubic and hexagonal semiconductor materials.

Introduction

Traditionally, MC simulation programs are written in an imperative programming language, most typical Fortran77, for a specific problem or a small class of problems. Adaptations to other kinds of problems, and even minor adjustments, involve programming work and often a considerable part of this work is due to shortcomings in the basic program design. These limitations regarding the kind of problems handled by a simulator are caused by the following facts:

---

[1]Speaker; e-mail: `Mats.Hjelm@ite.mh.se`

[2]also: Solid State Electronics, Department of Microelectronics and Information Technology, Royal Institute of Technology (KTH), Electrum 229, SE-164 40 Kista, Sweden

- The immense number of possible combinations of interacting submodels.

- The relatively poor modelling capability of imperative programming languages.

- The simulation packages are developed as part of research projects, where it is more important to present fast results than develop a stable platform for future projects. Until now there has been very little commercial interest in MC simulators that could motivate the investment in a general MC software.

- The tradition in the physics and semiconductor physics community, where Fortran and C are well known languages, but the knowledge of object-oriented languages is very poor.

The goal for a project developing a general MC simulator must be a software package, where all necessary models are available in the package. The users should only specify the characteristics of the semiconductor material and of the simulated device, combining the adequate submodels for the actual simulation. Furthermore, data for non-related submodels have to be cleanly separated in different files, so that for instance material data tested in bulk simulations can be used in device simulations without any change. The complexity of the problem is such that the simulator must be written in object-oriented style, and a language giving full support of object-orientation is highly recommendable. In order to handle the huge variation of sizes of the necessary data structures, it is also necessary to make extensive use of dynamic data structures.

An interesting aspect of this kind of projects is the development process. First of all, it is only feasible if there is a fundamental understanding of the importance of generality. Secondly, the software has to be continuously used in scientific "production" simulations. These simulations have to start with one specific material and some relatively simple devices. To achieve the generality it is then necessary to make successive amendments to the program. Many of them will result in the need to remodel older parts of the program, with accompanying testing and debugging. This kind of process, known as incremental and iterative program development, is tedious and the use of an object-oriented method helps greatly to increase the reliability of the produced code.

IMPLEMENTATION

A general MC simulator has been developed based on the principles outlined above. The program handles cubic and hexagonal crystal symmetries. New crystal symmetries can be included by the addition of a small number of virtual functions and constant data areas. Besides the usual MC simulation, the program contains modules for precalculation of energy or k-vector dependent scattering rates, density of states, q-vector dependent dielectric function and impact ionization transition rates from the full band structure.

The MC device simulator allows the description of arbitrary device geometries and doping profiles. In addition, our implementation allows the device to be subdivided into different regions, each with its proper material model. Furthermore, there is no arbitrary limitation in the number of regions. The region concept can hence be used for a large number of different purposes, which may range from simulation of different temperatures, over the usage of simplified models in high-doped areas, to simulation of heterostructures.

As an underlying structure for handling of statistic data and the discretization necessary for the solution of Poisson's equation, the simulator uses a mesh structure covering the entire device. The charge to mesh assignment uses a data driven approach, which allows the use of arbitrary charge assignment functions. Each mesh cell is also used to define a local weight factor for the superparticles, diminishing the number of them in high-doped areas. The scaling is made dynamically joining and splitting the superparticles according to the cell weight factor. This approach results in considerably faster simulation time.

The efficiency and flexibility of the described approach is demonstrated in simulations of MOSFET and MESFET devices in Si and 4H-SiC.

Hee Sun Regina Hong
Department of Mathematics
Hong Kong Baptist University
Kowloon Tong, Hong Kong
e-mail: `hshong@math.hkbu.edu.hk`

Fred J. Hickernell
Department of Mathematics
Hong Kong Baptist University
Kowloon Tong, Hong Kong
e-mail: `fred@math.hkbu.edu.hk`

TITLE

Distributions of the Discrepancy of Scrambled Digital (λ, t, m, s)-Nets

ABSTRACT

Art Owen proposed scrambled (t, s)-sequences as a hybrid of Monte Carlo and quasi-Monte Carlo methods. Quasi-Monte Carlo methods which use low discrepancy sequences often yield a higher convergence rate than Monte Carlo methods. However, Monte Carlo methods facilitate easier error estimate which is difficult for quasi-Monte Carlo methods. Randomizing quasi-Monte Carlo methods obtain the benefits from the best of both by yielding higher accuracy with practical error estimates.

Here we use a variation of Art Owen's random scrambling which is not as general as his, but still retains most of the desired properties. The following describes the construction of randomly scrambled digital (λ, t, m, s)-nets.

Let $b \geq 2$ denote a prime power, and let $\mathbf{Z}_b = \{0, 1, \ldots, b - 1\}$ be the finite (Galois) field of order b. For any non-negative integer $i = \cdots i_3 i_2 i_1 (\text{base } b)$, define the $\infty \times 1$ vector $\boldsymbol{\psi}(\boldsymbol{i})$ as the vector of its digits. Let $\mathbf{C}_1, \ldots, \mathbf{C}_s$ denote predetermined $\infty \times \infty$ *generator matrices*. Let $\mathbf{L}_1, \cdots, \mathbf{L}_s$, be nonsingular lower triangular $\infty \times \infty$ matrices with non-zero diagonal entries and let $\mathbf{e}_1, \cdots, \mathbf{e}_s$ be an $\infty \times 1$ vector. Assume that for all r any linear combination of columns of $\mathbf{L}_r \mathbf{C}_r$ plus $\mathbf{e}_r$ does not end in an infinite trail of $b-1$. A particular Owen-scrambled sequence, $\{\mathbf{x}_i\}$, is defined as

$$\boldsymbol{\phi}(\boldsymbol{x_{ir}}) = \mathbf{L}_r \mathbf{C}_r \boldsymbol{\psi}(\boldsymbol{i}) + \mathbf{e}_r, \quad r = 1, \ldots, s, \ i = 0, 1, \ldots. \tag{1}$$

Here all arithmetic operations take place in the finite field $\mathbf{Z}_b$. To get a randomly scrambled sequence one chooses the elements of the $\mathbf{L}_r$ and $\mathbf{e}_r$ randomly. A non-scrambled sequence is obtained by choosing $\mathbf{L}_1 = \cdots = \mathbf{L}_s = \mathbf{I}$ and $\mathbf{e}_1 = \cdots = \mathbf{e}_s = 0$.

For an integer λ, $1 \leq \lambda \leq b - 1$ the set of pints $\{x_0, \cdots, x_{\lambda b^{m-1}-1}\}$ is a digital (λ, t, m, s)-net. The t-value for the digital sequence depends on the generator matrices $\mathbf{C}_r$.

The discrepancy measures the uniformity of the distribution of a set of points and can be interpreted as the maximum possible quadrature error over a unit ball of integrands. Here we examine the distribution of the discrepancy for scrambled digital nets. The following is the discrepancy that we used here.

$$D(\{\mathbf{x}_i\})^2 =$$
$$-1 + \frac{1}{N^2} \sum_{i,j=0}^{\lambda b^m - 1} \prod_{r=1}^{s} \left[-\frac{(-\gamma^2)^\alpha}{(2\alpha)!} B_{2\alpha}(\{x_{ir} - x_{jr}\}) + \sum_{k=0}^{\alpha} \frac{\gamma^{2k}}{(k)^{2}!} B_i(x_{ir}) B_i(x_{jr}) \right]$$

134

where $B_i(x)$ are Bernoulli polynomials, and the notation$\{x\}$ means the fractional part of a number of vector x. The positive integer α indicates the degree of smoothness of integrands in the underlying Hilbert space, and the parameter γ measures the relative importance given to the uniformity of the points in low dimensional projections of the unit cube versus high dimensional projections of the unit cube.

Numerical experiments have been performed to compute empirical distribution of three different scrambled (λ, t, m, s)-nets, namely Sobol', Niederreiter-Xing, and a new sequence, where the generator matrices are obtained by using an evolutionary algorithm. The discrepancy of simple random points is computed also. Computations have been performed with different dimensions, numbers of points, and different γ values. Comparisons of the empirical distributions and their implications are discussed.

K. Kalna [1]
A. Asenov [2]
Device Modelling Group
Department of Electronics & Electrical Engineering
University of Glasgow
Oakfield Avenue
G12 8LT Glasgow
e-mail: `kalna@elec.gla.ac.uk`
`http://www.elec.gla.ac.uk/∼kalna/`

Title

Nonequilibrium and Ballistic Transport, and Backscattering in Decanano HEMTs: A Monte Carlo Simulation Study

Abstract

High electron mobility transistors (HEMTs) can be scaled into decanano dimensions in an effort to attain better performance in RF applications. As the device dimensions are reduced, the nonequilibrium and, particularly, ballistic transport starts to play an important role. This paper investigates electron transport in a set of aggressively scaled HEMTs using Monte Carlo (MC) device simulations. The study is based on an enhanced electron Monte Carlo transport model embedded in our finite element simulator H2F. A thoughtful calibration of the simulator has been performed against real 120 nm gate length pseudomorphic HEMTs. The scaling of HEMTs is considered both in lateral and transversal directions in respect to gate lengths of 90, 70, 50 and 30 nm. The scaled devices exhibit dramatic improvement in performance although the external parasitics exert limitations (1). In addition, we also investigate scaled HEMTs in which a second delta doping layer has been introduced into the device structure (2). Placement of the second delta doping below the channel improves the device linearity whereas placing the second delta doping above the original delta layer, near to the gate, can improve transconductance (3).

The detailed study of the nonequilibrium transport in the scaled devices requires monitoring of the velocity of each carrier through the device during the MC simulation thus enabling the determination of the average carrier velocity. The average particle velocity in the channel increases rapidly when the PHEMT is scaled from 120 to 70 nm in both single and double doped structures. However, the velocity saturates with the further scaling of the devices to gate lengths of 50 and to 30 nm. Electron transport in the channel beneath the gate has a highly non-equilibrium character. The average particle velocity achieves its peak value here and this is much larger than the bulk saturation velocity. A sharp drop in the velocity is observed when electrons reach the extremely high field recess region on the drain side of the device.

We have also compared the average particle velocities in the single and double doped structures. The peak of the average velocity through the channel is always larger in the double

---

doped HEMTs than in the single doped HEMT. The peak velocity is larger by 10-20% in the devices with the additional delta doping below the channel but only by 2-5% in the devices with the second doping layer above the original doping. It appears that the effective gate length in the double doped PHEMT with the second delta doping below the channel is the same as the length in the single doped structure. However, the effective gate length in the double doped PHEMT with the additional delta doping above the original doping is greater. These observations suggest that the second delta doping layer placed below the channel, which increases the carrier sheet density in the device by about 70%, improves electron transport in the channel. These devices exhibit a larger device linearity but no improvement in transconductance. The double doped HEMT with the additional delta doping close to the gate exhibits an increase in transconductance even the peak average velocity is practically the same as in the single doped structure. This fact tell us that this increase in transconductance comes solely from the better gate control of the charge in the channel (4).

The device gate length of the decanano PHEMTs becomes comparable to the inelastic mean-free path of the carriers. Hence, electrons travelling through the gate region should have a high probability of passing through this region ballistically (without suffering any collisions). To study the ballistic transport in the scaled devices we monitor particles in the gate-controlled-channel region and then calculate a field-momentum relaxation time as a reciprocal of Γ_{fm},

$$\Gamma_{\mathrm{fm}} = \frac{e}{\hbar} \frac{|\mathbf{F}|}{|\mathbf{k}|} \ ,$$

where $\mathbf{F}$ is the electric field vector at the particle position and $\mathbf{k}$ is the particle wavevector. This relaxation time represents the time during which the absolute particle momentum is relaxed due to the effect of the electric field at the particle position. The field-momentum relaxation rate, Γ_{fm}, is averaged over the number of particles passing through the gate-channel region to give the mean field-momentum relaxation rate.

The mean field-momentum relaxation time can be compared among different devices in order to assess the typical transport situation in the selected region of a device. When the field-momentum relaxation time increases a large number of carriers can travel ballistically due to the high electric fields and the small amount of scattering. On the other hand, a decrease of this relaxation time clearly indicates that carriers undergo many scattering events in the selected device region even if high electric fields are present. Using the field-momentum relaxation time as one of the device characteristic parameter can, with the help of all other information acquired by MC simulations of the transport in semiconductor devices, expose the ballistic limit (6) which is expected as a result of the scaling process.

The mean field-momentum relaxation time increases with the gate scaling only up to the 90 nm gate length device in accordance with the behaviour of the average velocities in the channel and then drops down to 50 nm and saturates at 30 nm device. This can be explained as follows. The effect of the gate-fringing plays a significant role in particle kinetics (5). The impact of this effect on particles increases when the gate length is scaled down. The huge electric field in the recess region surrounds the gate and, consequently, the particles are accelerated by these fringing fields when leaving the gate region on the drain side. The acceleration by the gate-fringing effect, however, is limited in devices with gate lengths less than 90 nm. This limitation is imposed by the increased scattering with phonons at high

energies which mainly results in backscattering (6). As a result, the mean field-momentum relaxation time starts to drop rapidly and then saturates when the gate length is scaled from 50 to 30 nm. The saturation of the field-momentum relaxation time occurs as the field particle acceleration and energy losses as a result of the increased backscattering become balanced. Backscattering adversely affects device performance and neutralises the benefits of ballistic transport.

References

[1] K. Kalna, S. Roy, A. Asenov, K. Elgaid, and I. Thayne, "RF analysis of aggressively scaled pHEMTs", in *Proceedings of ESSDERC 2000*, ed. by W. A. Lane, G. M. Crean, F. A. McCabe and H. Grünbacher (2000) 156-159.; K. Kalna, A. Asenov, K. Elgaid, and I. Thayne: "Scaling of pHEMTs to decanano dimensions" accepted to VLSI design (2001).

[2] K. Y. Hur, K. T. Hetzler, R. A. McTaggart, D. W. Vye, P. J. Lemonias, and W. E. Hoke: "Ultralinear double pulse doped AlInAs/GaInAs/InP HEMTs", Electron. Lett. **32** (1996) 1516-1518.

[3] K. Kalna and A. Asenov: "Multiple delta doping in aggressively scaled PHEMTs" submitted to ESSDERC 2001.

[4] I. C. Kizilyalli, M. Artaki, N. J. Shah, and A. Chandra: "Scaling properties and short-channel effects in submicrometer AlGaAs/GaAs MODFET's: A Monte Carlo study", IEEE Trans. Electron Devices **40** (1993) 235-249.

[5] J. Han and D. K. Ferry: "Scaling of gate length in ultra-short channel heterostructure field effect transistors", Solid-State Electron. **43** (1999) 335-341.

[6] M. Lundstrom, Z. Ren and S. Dutta: "Essential physics of carrier transport in nanoscale MOSFETs," *Proceedings of SISPAD'00*, ed. by J. Faricelli and P. Leon (Seattle, U.S.A., 2000) 1-5.

Phelim P. Boyle
Adam W. Kolkiewicz
Ken Seng Tan
University of Waterloo
Waterloo, Ontario N2L 3G1
Canada

TITLE

Pricing American Style Options Using Low Discrepancy Sequences

ABSTRACT

Monte Carlo simulation is an important computational tool for pricing complex derivatives and valuing real options. It is widely used in modern risk management since it is well suited for dealing with the large number of variables that are required to analyze the market risk and credit risk of large portfolios. The two most important limitations of the Monte Carlo method are that it is slow and the pricing of American options is difficult for high dimensional problems. For a review and a discussion of related issues, see Boyle et al. (1997).

Until the publication of Tilley's 1993 paper it was believed that American options could not be valued by Monte Carlo simulation. Since then, this problem has attracted considerable academic attention but despite significant progress has not been adequately solved for high dimensional problems. The problem can be set up in a dynamic programming framework where we can solve the optimization problem by working backwards through time. However in the standard Monte Carlo method we generate future price paths of the asset or assets in question starting from the current time. This forward marching approach clashes directly with the backward recursion feature of dynamic programming. The decision to exercise depends on the topography of the early exercise boundary, which is not furnished by standard Monte Carlo methods used for European options.

In Boyle et al. (2000) we have introduced a new version of the Monte-Carlo method for pricing high-dimensional American style derivatives. For these options, the estimation of the decision rule to exercise early is equivalent to the estimation of a series of conditional expectations with respect to different distributions. We propose to approximate these expectations by sampling at each time step from only one distribution. We formulate optimality criteria for this distribution and solve them. As it is not easy to use the optimal solution in practice, we propose some approximations and show their asymptotical optimality. This approach allows us to utilize quasi-Monte Carlo techniques, and we demonstrate that the resulting biased high estimator achieves the high rate of convergence typical for low discrepancy sequences.

In this paper, we extend the previous work by proposing another estimator that is biased low. It has the computational advantage that it can be obtained concurrently with the high-biased estimator using recursive valuation approach.

The new estimator is a modification of the one considered by Avramidis et al. (2000) in the context of a stochastic mesh only. Although low discrepancy sequences can also be applied to the latter, the one that we propose exhibits a superior rate of convergence.

Unlike the bias high estimator, we prove that the new estimator is only asymptotically bias low. However, as we demonstrate, this does not cause serious practical problems if the estimator is used jointly with low discrepancy sequences.

Some numerical examples are conducted to demonstrate efficiency of the method. We also show that further enhancement to the proposed estimator is possible by incorporating some of the standard variance reduction techniques.

References

[1] T. Avramidis, Y. Zinchenko, T.F. Coleman and A. Verma. Efficiency improvement for pricing American options with a stochastic mesh: Parallel implementation. Working paper, Cornell University, 2000.

[2] P.P. Boyle, M. Broadie, and P. Glasserman. (1997) Monte Carlo methods for security pricing. *Journal of Economic Dynamics and Control*, 21:1267–1321.

[3] P.P. Boyle, A. Kolkiewicz, and K.S. Tan. (2000) Pricing American style options using low discrepancy mesh methods. Technical report, IIPR 00-07, University of Waterloo.

[4] J. A. Tilley. Valuing American options in a path simulation model. (1993) *Transactions of the Society of Actuaries*, XLV:499–520.

Hans Kosina [1]
Institute for Microelectronics
TU-Vienna
Gußhausstraße 27-29/E360
A-1040 Vienna, Austria
e-mail: `Kosina@TUWien.ac.at`
`http://www.iue.tuwien.ac.at`

Title

An Event Bias Technique for Monte Carlo Device Simulation

Abstract

Monte Carlo (MC) simulation of semiconductor devices requires measures to enhance the statistics in phase space regions of interest that are sparsely populated. There are two general classes of statistical enhancement techniques, namely population control techniques and event bias techniques (1). To date virtually all MC device simulation codes utilize population control techniques, whereas the event bias technique, introduced in the field of semiconductor transport only one decade ago, (2)(3), has found no application.

This work deals with the MC method for stationary carrier transport, known as the Single-Particle MC method. It gives a solution to the stationary boundary value problem defined by the semi-classical Boltzmann equation. A theoretical analysis of this MC algorithm begins with the transformation of the stationary Boltzmann equation into an integral equation (4). Because the obtained equation describes the evolution back in time and we are aiming at a forward MC algorithm, the conjugate equation needs to be formulated. The elements of the Neumann series of the conjugate equation are finally evaluated by means of MC integration (4). Using this mathematically-based approach the Single-Particle MC method is derived in a formal way. For the first time, the independent, identically distributed random variables of the simulated process are identified, allowing to supplement this MC method with the natural stochastic error estimate. Furthermore, the extension of the MC estimators to the case of biased events is derived.

The kernel of the conjugate equation yields the natural probability distributions which are used for the construction of the particle trajectory. However, it is possible to choose other than the natural probabilities for the MC integration of the terms of the Neumann series. In that case one constructs numerical trajectories that differ from the physical ones. The motivation for using arbitrary probabilities is the possibility to guide particles towards a phase space regions of interest to enhance statistics. In this work we increase carrier diffusion against a retarding electric field by introducing artificial carrier heating. The probability for phonon absorption is increased at the expense of phonon emission, a measure which increases the probability of a numerical particle to surmount an energy barrier. In regions with small field, where transport is diffusion dominated, the distribution of the scattering

angle is biased so as to induce artificial carrier diffusion. Furthermore, the distribution at the boundaries has been modified, injecting test particles at much higher temperature than the lattice temperature.

Changing probability distributions requires compensatory changes in the estimators. The event bias technique can be summarized by a simple rule. Whenever in the course of numerical trajectory construction a random variable, for example, a free flight time or an after scattering state, is selected from a numerical density rather than from a physical density, the weight of the test particle changes by the ratio of the physical over the numerical density. As a consequence, the weight of a test particle evolves randomly. Individual particle weights can evolve to extremely different values, predominantly to very small ones.

Optimal values of the parameters which control the bias are not known a priori. If the bias is chosen too small, not enough particles will, for example, surmount an barrier, rendering statistical enhancement inefficient. On the other hand, by choosing the bias too large numerous numerical trajectories will pass through the low concentration region. However, due to the aggressive biasing the spreading of the particle weights will be very large, and the recorded averages will again show a large variance. To find some optimum between these two extreme cases a careful tuning of the bias parameters is necessary.

The described behavior of the event bias scheme suggests the usage of additional variance reduction techniques (5). In the presented simulation study evolution of the particle weight is governed predominantly by the event bias technique, and explicit measures are taken only to prevent particle weights from getting extremely high or low (6).

The formal approach, which is based on Monte Carlo integration of the terms of the Neumann series, clearly shows what the independent, identically distributed random variables are. A realization of such random variable is a complete numerical trajectory that starts and terminates at the domain boundary. Only complete numerical trajectories can be considered independent from each other, whereas particle states generated on one trajectory are statistically dependent. Knowing these random variables standard textbook formulae can be applied to estimate the variance of the MC estimates (7).

References

[1] M. Gray, T. Booth, T. Kwan, and C. Snell, "A Multicomb Variance Reduction Scheme for Monte Carlo Semiconductor Simulators," *IEEE Trans.Electron Devices*, vol. 45, no. 4, pp. 918–924, 1998.

[2] C. Jacoboni, "A New Approach to Monte Carlo Simulation," in *Int.Electron Devices Meeting*, (Washington, D.C.), pp. 469–472, IEEE Electron Devices Society, 1989.

[3] M. Nedjalkov and P. Vitanov, "Application of the Iteration Approach to the Ensemble Monte Carlo Technique," *Solid-State Electron.*, vol. 33, no. 4, pp. 407–410, 1990.

[4] H. Kosina, M. Nedjalkov, and S. Selberherr, "Theory of the Monte Carlo Method for Semiconductor Device Simulation," *IEEE Trans.Electron Devices*, vol. 47, no. 10, pp. 1898–1908, 2000.

[5] C. Wordelman, T. Kwan, and C. Snell, "Comparison of Statistical Enhancement Methods for Monte Carlo Semiconductor Simulation," *IEEE Trans.Computer-Aided Design*, vol. 17, no. 12, pp. 1230–1235, 1998.

[6] H. Kosina, M. Nedjalkov, and S. Selberherr, "Variance Reduction in Monte Carlo Device Simulation by Means of Event Biasing," in *Proc. Modeling and Simulation of Microsystems, MSM 2001* (M. Laudon and B. Romanowicz, eds.), pp. 11–14, Computational Publications, Mar. 2001.

[7] H. Kosina, M. Nedjalkov, and S. Selberherr, "Variance and Covariance Estimation in Stationary Monte Carlo Device Simulation," in *Proc. Simulation of Semiconductor Processes and Devices*, (Athens, Greece), Sept. 2001.

Timothy N. Langtry [1]
Lindsay C. Botten
Department of Mathematical Sciences
University of Technology, Sydney
NSW 2007, Australia
e-mail: `Tim.Langtry@uts.edu.au`
e-mail: `Lindsay.Botten@.uts.edu.au`

Ara A. Asatryan
Ross C. McPhedran
School of Physics
University of Sydney
NSW 2006, Australia
e-mail: `ara@physics.usyd.edu.au`
e-mail: `r.mcphedran@physics.usyd.edu.au`

TITLE

Monte Carlo and Quasi-Monte Carlo Modelling of Photonic Crystals [2]

ABSTRACT

In this paper we describe the application of Monte Carlo simulation to the modelling of photonic crystals, a new class of materials with optical properties that offer promise in a range of potential applications in the areas of information and communications technology. First we describe the relevant physical and structural properties of these materials and outline the derivation of the corresponding theoretical model. We then describe a Monte Carlo investigation of the tolerance of these materials to fabrication defects.

Photonic crystals are a novel type of optical material in which the refractive index varies periodically with position, which through interferometric action yields photonic band gaps— that is, ranges of frequencies for which electromagnetic waves cannot propagate within the structure. Defects in the material or structural properties of the crystal give rise to localised states, or field modes, analogous to the impurity modes of semiconductors. These change the radiation dynamics of the crystal and provide the ability to mould the flow of light in various ways. It is this property that gives rise to many significant applications, including the fabrication of microscopic lasers, new families of optical fibres, and the fabrication of optical waveguides and switches which may be used as components in future integrated photonic circuits.

Much of the research to date has been devoted to development of methods to compute transmission spectra and the related band diagrams that characterise the frequencies and directions for which light may propagate within a crystal. These, however, provide little insight into their radiation dynamics, which are characterised by the *local density of states* (LDOS). In three-dimensional crystal structures, for a given frequency the LDOS provides the spectral distribution of modes to which a fluorescent source can couple. For large LDOS values, emission at that frequency is enhanced; correspondingly, a small LDOS value indicates that light emission is suppressed.

To date, the LDOS has been calculated in infinite periodic structures of one dimension, and at isolated points within the unit cell of a three-dimensional lattice of spheres. Because of

---

[1]Speaker

the infinite extent of these structures, the LDOS vanishes identically within band gaps. For realistic structures of finite extent, however, the LDOS within a band gap does not vanish and it is thus a parameter of physical significance for photonic applications. Accordingly, there is considerable interest in the development of efficient methods for computing densities of states, and related measures, for finite crystals of realistic size.

In this paper we compute the two-dimensional LDOS for a two-dimensional crystal comprising a finite cluster of N_c infinite circular cylinders aligned with the z axis, with cylinder l centred at $\mathbf{c}_l$ and having radius a_l and refractive index n_l. The LDOS $\rho(\mathbf{r}; \omega)$ is a function of spatial position $\mathbf{r}$ and temporal angular frequency ω that is defined by

$$\rho(\mathbf{r}; \omega) = -\frac{2\omega}{\pi c^2} \Im \mathrm{Tr} \left[\mathbf{G}^e(\mathbf{r}, \mathbf{r}; \omega) \right],$$

in terms of the electromagnetic Green's tensor $\mathbf{G}^e(\mathbf{r}, \mathbf{c}_s; \omega)$, in the limit that the source position $\mathbf{c}_s$ approaches the field (observation) point $\mathbf{r}$. The Green's tensor represents the field response due to a line source (in two dimensions) and, in the case of in-plane incidence, the field problem decouples into its two fundamental polarisations in which either the electric or magnetic fields align with the cylinder axis. These are respectively referred to as transverse magnetic (TM) or transverse electric (TE) polarisations.

For simplicity and brevity, we outline only the treatment for TM polarisation that is parametrised by the single non-trivial component of $\mathbf{G}^e$, i.e., $V^e \stackrel{\text{def}}{=} G^e_{zz}$ satisfying the boundary value problem

$$\nabla^2 V^e(\mathbf{r}; \mathbf{c}_s) + k^2 n^2(\mathbf{r}) V^e(\mathbf{r}; \mathbf{c}_s) = \delta(\mathbf{r} - \mathbf{c}_s), \tag{1}$$

in which V^e and its normal derivative $\nu \cdot \nabla V^e$ at any interface are everywhere continuous. Here, k is the free-space wavenumber and $n(\mathbf{r})$ denotes the refractive index.

In the vicinity of each cylinder l, the exterior field in the free space background is expanded in local coordinates $\mathbf{r}_l = (r_l, \theta_l) = \mathbf{r} - \mathbf{c}_l$,

$$V^e(\mathbf{r}; \mathbf{c}_s) = \sum_{m=-\infty}^{\infty} \left[A_m^l J_m(kr_l) + B_m^l H_m^{(1)}(kr_l) \right] e^{im\theta_l}, \tag{2}$$

and involves both irregular components, characterised by coefficients B_m^l, denoting scattered field sources associated with this cylinder, and regular components characterised by A_m^l.

The regular fields characterised by $\mathbf{A}$, arise from both sources $\mathbf{B}$ on all other scatterers and the radiation $\mathbf{K}$ due to the field source at $\mathbf{c}_s$. In matrix nomenclature in which the $\mathbf{A}$, $\mathbf{B}$ and $\mathbf{f}$ denote partitioned vectors, each partition of which contains coefficients in the cylindrical harmonic expansions (2) in the vicinity of each scatterer, it may be shown that

$$\mathbf{A} = \mathbf{SB} + \mathbf{K}, \tag{3}$$

a form that typifies the solution of problems formulated with multipole methods. In (3), $\mathbf{S}$ is a partitioned matrix specifying multipole contributions associated with sources on each scatterer.

Field continuity conditions on cylinder boundaries imply

$$\mathbf{B} = \mathbf{RA} + \mathbf{TQ}, \tag{4}$$

in which $\mathbf{R}$ and $\mathbf{T}$ denote matrices of cylindrical harmonic reflection and transmission coefficients, and $\mathbf{Q}$ represents a source interior to a cylinder. This, together with (3) leads to the field identity

$$(\mathbf{I} - \mathbf{RS})\mathbf{B} = \mathbf{RK} + \mathbf{TQ}, \tag{5}$$

a form that is particularly amenable to implementation on parallel systems.

To gain insight into the radiation dynamics of a photonic crystal it is necessary to compute the LDOS at a set of points in the crystal. The set may comprise a single point, or may sample the entire structure, yielding an LDOS map of the crystal. Of particular significance are the effects on the radiation dynamics of perturbations in the material and geometric properties, yielding insight into the tolerances acceptable in the manufacture of photonic crystals. In particular, we are interested in how sensitive the LDOS is to random perturbations in the positions of the scattering cylinders, their radii, and their refractive indices. A corresponding computational problem is to estimate the mean LDOS corresponding to random perturbations of these quantities with specified distributions. Monte Carlo simulation is used to estimate the mean LDOS corresponding to perturbations with given distributions. Let $\epsilon = (\epsilon_{\mathbf{r}}, \epsilon_{\mathbf{a}}, \epsilon_{\mathbf{n}})$ be a partitioned vector denoting a random perturbation of the positions, radii and refractive indices of the cylinders comprising the crystal. Denote by $\rho(\mathbf{r}, \epsilon; \omega)$ the LDOS of the perturbed crystal, by $\overline{\rho}(\mathbf{r}, \omega)$ the mean LDOS at $\mathbf{r}$ and ω of the perturbed crystals, and define the ensemble average of a sample of N_I perturbations by $\widehat{\rho}_{(N_I)}(\mathbf{r}; \omega) \stackrel{\text{def}}{=} \frac{1}{N_I} \sum_{j=1}^{N_I} \rho(\mathbf{r}, \epsilon; \omega)$. We apply a sequence of N_I pseudo-random perturbations to a given crystal structure, accumulating $\widehat{\rho}_{(N_I)}(\mathbf{r}; \omega)$ at each point $\mathbf{r}$ of interest. Figure 1 gives both surface and contour plots of $\widehat{\rho}_{(40)}$ for a crystal design containing a waveguide. The frequency used lies in the band gap for the crystal and the positions of the cylinders are indicated by the circles in the contour plot. In this example, uniformly distributed perturbations of the cylinder radii were sampled, with a maximum deviation from the design value of 10% . The remaining design parameters were left unperturbed. The figure demonstrates the suppression of propagation within the structure except in the waveguide, indicating that the crystal possesses substantial guiding properties. A similar treatment with a maximum $33\frac{1}{3}\%$ variation in cylinder radii, however, demonstrates the loss of these properties.

Figure 1: Random variations of radii with maximum deviation 10% from the design value for the crystal.

Pierre L'Ecuyer
Jacinthe Granger-Piché [1]
Départment d'Informatique et de Recherche Opérationelle
Université de Montréal
C.P. 6128, Succ. Centr-Ville
Montréal, H3C 3J7, Canada
e-mail: `lecuyer@iro.umontreal.ca`
and: `granger@iro.umontreal.ca`
`http://www.iro.umontreal.ca/~lecuyer`

Title

Combining Generators from Different Families

Abstract

Combined random number generators with components of the same type (e.g., linear congruential or multiple recursive or Tausworthe) have been studied extensively, and specific generators of this form are now available in several software packages. The theoretical properties of these generators tend to be easy to analyze because of their highly regular structure. Having a lot of structure is convenient from the analysis viewpoint but can be seen as a drawback from the "apparent randomness" or "unpredictability" viewpoint. It is then interesting to explore how much understanding of the structure, and how much of the "guaranteed uniformity" of the point set produced by the generator over its full period, must be given away in order to obtain a more complicated (or less regular) structure.

In this talk, we discuss the combination of generators from different families (e.g., a linear congruential with a Tausworthe, or a linear generator with a nonlinear one), from the theoretical and empirical viewpoints. We consider the following two main classes of combinations: (a) a linear congruential or multiple recursive generator (LCG or MRG) combined with another type of generator by adding the outputs modulo 1, and (b) a linear feedback shift register (LFSR) generator combined with another type of generator via a bitwise exclusive-or.

We analyze the structural proprieties of the set Ψ_t of all overlapping t-tuples of successive output values from these combined generators. We show that a certain level of uniformity for this set can be guaranteed if the points produced by the LCG, MRG or LFSR are well distributed in t dimension. On the other hand, these point sets Ψ_t have a much less regular structure than the corresponding point sets for generators from the LCG, MRG, or LFSR families alone. This shows up in empirical testing: Standard statistical tests require a much larger sample size to detect the structure (or to find statistical deficiencies of the generator) for a mixed combined generator than for a simple linear generator of comparable period length. According to our experiments, this trend is remarkably systematic.

After summarizing our empirical results, we will suggest specific mixed combined generators having efficient implementations.

Christiane Lemieux
Department of Mathematics and Statistics,
University of Calgary,
2500 University Drive N.W.,
Calgary (Alberta), Canada
e-mail: `lemieux@math.ucalgary.ca`

Pierre L'Ecuyer
Départment d'Informatique et de
Recherche Opérationelle
Université de Montréal
C.P. 6128, Succ. Centr-Ville
Montréal, H3C 3J7, Canada
e-mail: `lecuyer@iro.umontreal.ca`
`http://www.iro.umontreal.ca/~lecuyer`

Title

Polynomial Lattice Rules for Quasi-Monte Carlo

Abstract

Linear recurrences modulo 2 are widely used for constructing (pseudo)random number generators: Tausworthe and GFSR generators, twisted GFSRs, and Mersenne twisters are notable examples. Here, we use them for quasi-Monte Carlo integration over the unit hypercube, finite or infinite dimensional. Any stochastic simulation fits this framework. The idea is to choose a recurrence with a short period length and to estimate the integral by the average value of the integrand over all vectors of successive output values produced by the small generator, over all of its cycles. Combined generators and additional linear output transformation (tempering) can be used to improve the equidistribution of this point set.

We examine randomizations of this scheme, discuss criteria for selecting the parameters, and provide examples. This approach can be viewed as a polynomial version of ordinary lattice rules for multivariate integration. Essentially all of the developments and results that have been obtained in the context of ordinary lattice rules have their counterparts for the polynomial version. In particular, for a certain type of randomization, a variance expression for the integral estimator can be obtained in terms of the sum of squared Walsh coefficients of the integrand over the dual (polynomial) lattice. This suggests specific selection criteria (or figures of merit) for the lattice. According to our experiments, randomized polynomial lattice rules can provide significant variance reductions compared with the standard Monte Carlo method, even for large-dimensional problems (at least in some practical situations).

Gunther Leobacher
Friedrich Pillichshammer
Department for Financial Mathematics
University of Linz
Altenbergerstrasse 69
A-4040 Linz, Austria
e-mail: `Gunther.Leobacher@jk.uni-linz.ac.at`
`Friedrich.Pillichshammer@jk.uni-linz.ac.at`

TITLE

Sampling from the Hyperbolic Distribution

ABSTRACT

The hyperbolic distribution was introduced by O. E. Barndorff-Nielsen in 1977 in connection with the study of particle sizes. It has been observed by E. Eberlein and U. Keller in 1995 that the hyperbolic distribution is superior to the normal distribution in modelling the logarithmic rates of returns of a stock. The most important advantage of the hyperbolic distribution is that it has heavy tails compared to the normal distribution. This obviously makes big changes in market prices more likely and therefore leads to a more realistic model than the normal model.

In most cases, if one wants to sample from a distribution given by a density, one uses so called rejection algorithms. Though these methods work well for (pseudo) random point sets, they are not suited for the use of low discrepancy point sets, because they (as suggested by their name) abandon some points from the sample, thereby destroying the structure of the point set.

Still we want to use low discrepancy point sets, since they promise better performance, that is, faster convergence than Monte Carlo at least in low dimensions.

A much more direct approach for sampling from a given distribution is the inversion method: Let F be a continuous, strictly increasing distribution function. Let G denote its inverse function on (0,1). Then we can generate a random variable with distribution F by taking a uniformly distributed random variable U and applying G.

So if we want to generate random numbers with hyperbolic distribution, all we have to do is to find the inverse of the distribution function of the hyperbolic distribution and apply it to a uniformly distributed sample. This, however, is no trivial task, since neither the distribution function nor its inverse can be expressed in terms of elementary functions.

It is the objective of our paper to give a practically useful approximation to the inverse function of the hyperbolic distribution function. By "practical" we mean that samples with realistic sample sizes (e.g. 10 000 - 10 000 000) cannot be distinguished from "real" hyperbolic samples with the help of statistical tests.

For the statistical test on distribution we take the Kolmogorov-Smirnov test. The reason for this choice is that it relates the quality of our hyperbolic sample to the one-dimensional star-discrepancy of the underlying uniformly distributed sample.

Naturally, the difficulties in finding a good approximation to the inverse of the hyperbolic distribution function arise near the points 0 and 1. We find a good (or better: good enough) approximation for these domains and show how they can be glued together with a numerical solution (found with the help of e.g. Mathematica) in the center.

Gerhard Derflinger
Josef Leydold [1]
Günter Tirler
University of Economics and Business Administration
Department for Applied Statistics and Data Processing
Augasse 2-6, A-1090 Vienna, Austria
email: `Josef.Leydold@statistik.wu-wien.ac.at`

<small>TITLE</small>

Automatic Non-Uniform Random Variate Generation

<small>ABSTRACT</small>

In the last decades high quality generators for non-uniform random variates have been developed (see e.g. Devroye (1986), Dagpunar (1988), or (Fishman 1996) for surveys). However searching through the literature on simulation (e.g. Tyszer (1999)) or web based software repositories (like `http://gams.nist.gov/` or `http://www.netlib.org/`) one finds only simple generators. Even for the normal distribution one finds such infamous methods like the sum of 12 uniform random numbers (sic!). Moreover for problems as (e.g.) sampling from the truncated normal distribution there are often no algorithms provided. When generators for fairly uncommon distributions are required the help of an expert is necessary.

On the other hand universal (or black-box) methods have been developed to sample from large classes of distributions (see Leydold and Hörmann (2001) or Hörmann and Leydold (2000) for a short survey). They provide high quality generators even for non-standard distributions. However implementing such algorithms in a reliable and robust way result in rather complex programs. Installing and using such a program might seem too tedious for "just a random number generator".

The complexity of such programs arise from the setup and parts performing adaptive steps. The actual sampling routine is very simple. Thus such *automatic random variate generators* can also be used as *code generators*. The output of such a program is then a computer program in any high level programming language for the generator that samples from the desired distribution. This approach has the further advantage that it is possible to test the quality of random variates generated by the generated code.

The concept of an *Automatic Code Generator* for nonuniform random numbers can reduce the gap between theorists who create new algorithms and programmers or researches in different scientific areas who need state-of-the-art generators (or simply any generator for an uncommon simulation problem).

Using a web-based system it is even possible to avoid the troublesome installation of complex libraries. Looking for the right library function can be replace by filling out forms where the desired distribution can be selected from a menu or described by its probability density function given as ASCII-string, e.g., `max(1-x*x,0)`. Optional data about the distribution or the application of the generator can be added to the input form. The result is then a (short)

---

[1]Speaker

subroutine for a random variate generator coded in some high level programming language that can be used in ones program by simple cut & paste. A data file with the output of this generator can be appended to verify the code on the target maschine. Because every code is tested before printed on the screen the user is free of obscure error messages and program crashes that makes the usage of external code sometimes so tedious.

We have implemented such a system using the UNURAN library (Leydold, Hörmann, Janka, and Tirler 2001) for universal non-uniform random variate generators.

References

Dagpunar, J. (1988). *Principles of Random Variate Generation*. Oxford, U.K.: Clarendon Oxford Science Publications.

Devroye, L. (1986). *Non-Uniform Random Variate Generation*. New-York: Springer-Verlag.

Fishman, G. S. (1996). *Monte Carlo. Concepts, algorithms, and applications*. Springer Series in Operations Research. New York: Springer.

Hörmann, W. and J. Leydold (2000). Automatic random variate generation for simulation input. In J. A. Joines, R. Barton, P. Fishwick, and K. Kang (Eds.), *Proceedings of the 2000 Winter Simulation Conference*, pp. 675–682.

Leydold, J. and W. Hörmann (2001). Universal algorithms as an alternative for generating non-uniform continuous random variates. In G. I. Schuëller and P. D. Spanos (Eds.), *Monte Carlo Simulation*, pp. 177–183. A. A. Balkema. Proceedings of the International Conference on Monte Carlo Simulation 2000.

Leydold, J., W. Hörmann, E. Janka, and G. Tirler (2001). *UNU.RAN User Manual*. Augasse 2–6, A-1090 Wien, Austria: Institut für Statistik, WU Wien. available from `http://statistik.wu-wien.ac.at/unuran/`.

Tyszer, J. (1999). *Object-Oriented Computer Simulation of Discrete-Event Systems*. Boston, Dordrecht, London: Kluwer Academic Publishers.

Yiming Li
S. M. Sze
National Chiao Tung University and
National Nano Device Laboratories
P.O. Box 25-178, Hsinchu city
Hsinchu 300, Taiwan
e-mail: `ymli.ee87g@nctu.edu.tw`

Hsiao-Mei Lu
Inst. Statistics
Nat'l Tsing Hua Univ., Taiwan

Ting-Wei Tang
Dept. Electrical Computer Eng.
U. Mass., USA

Title

A Novel Parallel Adaptive Monte Carlo Method
for Nonlinear Poisson Equation in Semiconductor Devices

Abstract

A new Monte Carlo (MC) simulation technique for numerical solution of nonlinear Poisson equation in semiconductor device is presented. Based on fixed random walk algorithm, unstructured mesh technique, and monotone iterative method, this novel adaptive MC simulation of semiconductor nonlinear Poisson equation is proposed and successfully implemented on a 16-PCs Linux cluster with message-passing interface (MPI) library. The developed parallel MC Poisson solver tested on a submicron MOSFET device shows it has good efficiency and robustness. Furthermore, the implementation demonstrates that a well-designed load balancing MC simulation can reduce the execution time up to an order of magnitude. Benchmarks, such as speedup and efficiency are included to illustrate the excellent parallel performance of the method.

Conventional semiconductor device equations, such as drift diffusion, hydrodynamic and Boltzmann transport equations require solution of Poisson equation that describes the electrostatic potential distribution in the device for a specified doping profile (1). Many deterministic simulation methods, e.g., finite difference, finite element, finite volume, or boundary element methods have been developed to solve such nonlinear Poisson equation on 2D or 3D domain. However, they are unable to analyze efficiently some critical regions in a reasonable time because of the strong nonlinear behavior of Poisson equation and geometric complexity. In recent years, the MC method has been applied with great success in many disciplines, for example particle physics, quantum mechanics, heat conduction, electrical engineering, chemical reaction, and biology. This probabilistic technique could be economical when the solution within a small region is required in the simulation domain. It also has been found to be a very useful alternative for solving problems that have a sharp gradient near an interface, junction layer, or a boundary point. Various MC algorithms, such as fixed random walk, floating random walk, fixed-radius floating random walk, and Exodus methods have been proposed for the solution of linear electrostatic problems. These non-deterministic methods solve linear Poisson and Laplace equation in multi-dimensional rectangular, cubic, and spherical domains with highly computational accuracy and efficiency (2; 3; 4; 5).

In this paper, for the first time a new MC algorithm for the simulation of nonlinear Poisson equation in semiconductor device is proposed. The nonlinear Poisson equation is simulated with a fixed random walk algorithm, unstructured mesh technique, posteriori error estimation,

and monotone iterative methods. This novel approach has been successfully implemented on a 16-PCs Linux cluster with MPI library. First of all, the multi-dimensional nonlinear Poisson equation (1) is transferred into an iterative formulation (2) with monotone iterative technique $(1; 6)$

$$\Delta\phi = -\frac{q}{\varepsilon_S} \left(p\left(\phi\right) - n\left(\phi\right) + N_D^+ - N_A^- \right), \tag{6}$$

$$\Delta\phi^{(m+1)} + \lambda\phi^{(m+1)} = \\ -\frac{q}{\varepsilon_S} \left(p\left(\phi^{(m)}\right) - n\left(\phi^{(m)}\right) + N_D^+ - N_A^- \right) + \lambda\phi^{(m)}, \tag{7}$$

where the unknown to be solved is potential ϕ, $q = 1.60218 \times 10^{-19} C$ is the elementary charge, $\varepsilon_S = 11.9\varepsilon_0$ is silicon permittivity, n and p are densities of free electron and hole, respectively, N_D^+, and N_A^- are ionized donor and acceptor impurities, and $\varepsilon_0 = 8.85418 \times 10^{-14} \ F/cm$ is the permittivity in vacuum. The monotone iterative method has been successfully developed and applied to solve deterministically drift-diffusion and hydrodynamic semiconductor device simulations by us earlier $(7; 8; 9)$. The transferred nonlinear Poisson equation (2) is then solved with a fixed random walk algorithm for all initial grid points (see FIG. 1a). Because the strong nonlinear property of the Poisson equation, the mesh should be refined so that the final converged solution can be obtained efficiently. When a solution is computed (see FIG. 1b), we do a posteriori error estimation on the computed result for each mesh cell. If the error does not meet the tolerance, we refine the mesh. With this newer refined mesh, the Poisson equation is solved iteratively. The iterative loops will be terminated when a specified error criterion is reached. As shown in FIG. 2, the final refined mesh and computed solution present a very good computational efficiency of the new adaptive MC method. This method has good convergence behavior and it is easy for implementation and the algorithm is inherently parallel in large scale computing. The presented method has been successfully implemented on a 16-processors Linux-Cluster with MPI library. FIG. 3 shows the achieved parallel speedup for a tested submicron N-MOSFET at $V_{DS} = V_{GS} = 2V$.

A novel parallel Monte Carlo simulation for nonlinear Poisson equation in semiconductor device has been presented. Based on fixed random walk algorithm, unstructured mesh technique, a posteriori error estimation, and monotone iterative method, this novel approach has been successfully implemented on a 16-PCs Linux cluster with MPI library. The developed parallel MC Poisson solver tested on a submicron MOSFET device has shown it has good efficiency and robustness. Furthermore, the practical implementation demonstrates that a well-designed load balancing MC simulation can reduce the execution time up to an order of magnitude.

References

[1] S. M. Sze, Physics of Semiconductor Devices, 2nd Ed., Wiley-Interscience, New York, 1981.

[2] R. B. Iverson and Y. L. L. Coz, A Floating Random-Walk Algorithm for Extracting Electrical Capacitance, Math. Comp. Simulation, Vol. 55, pp. 59-66, 2001.

[3] R. C. Garcia and M. N. O. Sadiku, Neuro-Monte Carlo Solution of Electrostatic Problems, J. Franklin Inst. Vol. 335B, No. 1, pp. 53-69, 1998.

[4] J. M. Delanrentis and L. A. Romero, A Monte Carlo Method for Poisson's Equation, J. Comp. Phys., Vol. 90, pp. 123-140, 1990.

[5] M. N. O. Sadiku, Monte Carlo Solution of Axisymmetric Potential Problems, IEEE Trans. Indus. Appl. Vol. 29, No. 6, pp. 1042-1046, 1993.

[6] S. Heikkila and V. Lakshmikantham, Monotone Iterative Techniques for Discontinuous Nonlinear Differential Equations, Marcel Dekker, 1994.

[7] Y. Li, et al., Parallel Dynamic Load Balancing for Semiconductor Device Simulations on a Linux Cluster, ACR/IEEE Proc. Fourth Inter.Conf. Modeling and Simulation of Microsystem (MSM 2001), South Carolina, pp. 562-566, 2001.

[8] Y. Li, et al., "Adaptive Finite Volume Simulation of Semiconductor Devices on Cluster Architecture," in "Recent Advances in Applied and Theoretical Mathematics" Edited by N. Mastorakis, WSES Press, pp. 107-113, 2000.

[9] Y. Li, et al., A Novel Approach for the Two-Dimensional Simulation of Submicron MOS-FET's Using Monotone Iterative Method, IEEE Proc. Inter. Symp. VLSI-TSA, Taipei, pp. 27-30, 1999.

Sylvain Maire
Institut des sciences de l'ingnieur
de Toulon et du Var
Avenue Georges Pompidou bp 156
83162 La Valette du Var
France
e-mail: `maire@isitv.univ-tln.fr`

Title

A Fast Computation of L^2 Approximations with Monte Carlo

Abstract

In this paper we describe a new variance reduction method for Monte Carlo integration based on an iterated computation of quadratic approximations using control variates. This computation leads to non linear unbiased estimates for each of the coefficients of the finite L^2 expansion on D. They are built by computing a correction on the residue at each step of the algorithm using only sample values. We give estimations of the variance of these estimates without further assumptions on the approximation basis. We will see that the possible convergence of the algorithm depends mainly on constants $K(p) \leq p^2$ and $C(p)$ which are linked to integrals of a product of four terms of the approximation basis.

As a first application, we will study our algorithm for univariate regular functions. We will describe the quality of the approximation in the case of a decay as $\frac{C}{p^L}$ of the p coefficients of the quadratic approximation. We will first apply our algorithm to the Fourier expansion on periodised functions for which such a property holds. Then we will compute approximations using both Legendre and Tchebychef polynomials which satisfy the same property. Letting

$$f^{(M)}(x) = \sum_{k=1}^{p} a_k^{(M)} e_k(x)$$

the approximation of the finite expansion of f at the Mth step of the algorithm using N sample values by step, we will prove that

$$E(a_k^{(M)}) = <f, e_k>,$$

$$Var(a_k^{(M)}) \leq 2(\mu(p)\frac{1}{p^{2L-1}} + \mu_1 \frac{K(p)^{M-1}}{N^M}C(p)^M)$$

and also that

$$E(\int_D (f(x) - f^{(M)}(x))^2 dx) \leq 2p(\mu(p)\frac{1}{p^{2L-1}} + \mu_1 \frac{K(p)^{M-1}}{N^M}C(p)^M) + \mu_2 \frac{1}{p^{2L-1}}.$$

We will show furthermore that some of our estimates are not far to be optimal for C^k functions in a sense that their order are $0(N^{\frac{1}{2}-k-\varepsilon})$ compared to the optimal order which is $0(N^{-\frac{1}{2}-k})$ where N is the number of sample values. Numerical results will be given and compared to standard Monte Carlo integration.

We will then extend our method to the computation of multivariate L^2 approximations of regular functions. The crucial point in this extension is to take into account the dimensional effect. To do this, the choice of the elements of the approximation basis will be inspired from lattice rules methods which take advantage that the multidimensional Fourier coefficients a_m satisfy

$$|a_m| \leq \frac{c}{(\overline{m_1} \overline{m_2} ... \overline{m_Q})}$$

for all $m \in Z^Q$, where c is independent of m and $\overline{m} = \sup(|m|, 1)$. We will show that the same kind of decay also holds for Legendre and Tchebychef polynomial basis. For a given value of $d \in N$, we will only chose the $P_{Q,d}$ functions in the approximation basis which coefficients satisfy

$$\overline{m_1} \overline{m_2} ... \overline{m_Q} \leq d.$$

We will obtain Monte Carlo estimates which accuracy is quite similar to those obtained with lattice rules methods that is

$$Var(a_k^{(M)}) \leq 2(\mu_1 \frac{K(P_{Q,d})^{M-1}}{N^M} C(P_{Q,d})^M + \mu(P_{Q,d}) \frac{1}{d^{2L-1-\varepsilon}})$$

and also

$$E(\int_D (f(x) - f^{(M)}(x))^2 dx) \leq 2P_{Q,d}(\mu(P_{Q,d}) \frac{1}{d^{2L-1-\varepsilon}} +$$

$$\mu_1 \frac{K(P_{Q,d})^{M-1}}{N^M} C(P_{Q,d})^M) + \frac{\mu_2}{d^{2L-1-\varepsilon}}$$

The use of orthogonal polynomials allows to get rid of the artificial effects of periodisation on the constant c. We will also see that the version of our algorithm using Tchebychef polynomials is the most efficient because it reconcile the advantages of each of the other two basis: good accuracy and fast convergence. Numerical results will be comparable to those obtained with a numerical method developped in [1] that achieve the optimal order $0(N^{-\frac{1}{2} - \frac{k}{Q}})$ in the computation of Q-dimensional integrals. The main advantage of our algorithm toward this method is that it also gives a spectral approximation of the function with only a few terms. We will use this advantage by giving spectral approximations of integral form functions. We will also use it in the numerical solution of Fredholm integral equations of the second kind with regular kernels.

References

[1] E. I. ATANASSOV, I. T. DIMOV, A new optimal Monte Carlo method for calculating integral of smooth functions, Monte Carlo Methods and Appl., Vol. 5, No. 2, pp. 149-167 (1999).

[2] K. E. ATKINSON, The numerical solution of integral equations of the second kind, Cambridge university press, 1997.

[3] C. BERNARDI, Y. MADAY, Approximations spectrales de problmes aux limites elliptiques. Springer-Verlag. 1992

[4] A. R. KROMMER et C. W. UEBERHUBER. Computational integration. SIAM, 1998.

Chi-Ok Hwang
Michael Mascagni
Florida State University
203 Love Building, Tallahassee
FL 32306-4530, USA
e-mail: `hwang@cs.fsu.edu`
e-mail: `mascagni@cs.fsu.edu`

TITLE

A Feynman-Kac Path-Integral Implementation for Poisson's Equation Using an h-conditioned Green's Function

ABSTRACT

Since Müller proposed the "walk on spheres" (WOS) method for solving the Dirichlet boundary value problems for the Laplace equation, WOS has been a popular method. In addition, this random-walk based approach has been extended to solve other, more complicated, partial differential equations including Poisson's equation, and the linearized Poisson-Boltzmann equation. In WOS, instead of using detailed Brownian trajectories inside the domain, discrete jumps are made using the uniform first-passage probability distribution of the sphere. In this paper, this WOS method is combined with the Feynman-Kac formula to solve the Dirichlet boundary value problem for Poisson's equation.

Our implementation is based on the well-known Feynman-Kac representation of the solution to the Dirichlet problem for Poisson's equation. Recall that the Dirichlet problem for Poisson's equation is:

$$\frac{1}{2}\Delta u(\mathbf{x}) = -q(\mathbf{x}), \qquad \mathbf{x} \in \Omega \tag{1}$$

$$u(\mathbf{x}) = f(\mathbf{x}), \qquad \mathbf{x} \in \partial\Omega. \tag{2}$$

The solution to this problem, given in the form of the path-integral with respect to standard Brownian motion $X_t^{\mathbf{x}}$, is as follows:

$$u(\mathbf{x}) = E[\int_0^{\tau_D^{\mathbf{x}}} q(X_t^{\mathbf{x}})dt] + E[f(X_{\tau_D^{\mathbf{x}}}^{\mathbf{x}})]. \tag{3}$$

Here $\tau_D^{\mathbf{x}} = \{t : X_t^{\mathbf{x}} \in \partial\Omega\}$ is the first passage time and $X_{\tau_D^{\mathbf{x}}}^{\mathbf{x}}$ is the first passage location on the boundary, $\partial\Omega$.

Instead of simulating the detailed irregular motion of the Brownian trajectories, we use the h-conditioned Green's function for a ball with WOS as a probability density function. The h-conditioned Green's function gives the probability density distribution of the Brownian trajectory inside the ball during its passage from the center to the boundary. We construct a Brownian trajectory as a sequence of discrete jumps from ball centers to ball surfaces. By

using the h-conditioned Green's function, $K(\mathbf{x}, \mathbf{z})$, the first term of Eq. 3 for the ith ball of a WOS (Brownian) trajectory becomes:

$$\int_{B_i} q(\mathbf{x})K(\mathbf{x}, \mathbf{z})d\mathbf{x}. \tag{4}$$

Here, B_i is the ith ball and $\mathbf{z}$ is the first passage location on the surface of the ball, making the preceding a volume integral.

Eq. 4 readily permits the use of WOS to eliminate the need to compute the detailed Brownian trajectory. Instead, a series of discrete jumps in continuous space terminating on the boundary, $\partial\Omega$, is used. Jumping from ball to ball never permits a trajectory to land exactly on the boundary. Thus we use the standard WOS approach of "fattening" the boundary by ϵ to create a capture region that is used to terminate the walk. The error associated with this approximation has been theoretically estimated in previous WOS studies.

We wish to compute the solution to the Dirichlet problem for Poisson's equation at $\mathbf{x_0}$. For each Brownian trajectory starting at $\mathbf{x_0}$, with an ϵ-absorption layer, we accumulate the internal contribution for each ball and the functional value of the boundary condition at the final exit location on $\partial\Omega$. And so, an estimate for the solution at $\mathbf{x_0}$ is given by the statistic

$$S_N = \frac{1}{N}\sum_{i=1}^{N} Z_i, \tag{5}$$

where N is the number of trajectories and each statistic, Z_i, is given by

$$Z_i = \sum_{j=1}^{n_i}[\int_{B(\mathbf{x_j}, r_j)} q(\mathbf{x})K(\mathbf{x}, \mathbf{z})d\mathbf{x} + f(X_{\tau_D^{\mathbf{x}}}^{\mathbf{x}})]. \tag{6}$$

Here, n_i is the number of WOS steps needed for the ith Brownian trajectory to terminate in the ϵ-absorption layer, $\mathbf{x_j}$ is the center of the jth ball of radius r_j, and $X_{\tau_D^{\mathbf{x}}}^{\mathbf{x}}$ is the first passage location on the boundary, $\partial\Omega$.

We demonstrate our Feynman-Kac implementation by solving numerically a boundary value problem for Poisson's equation. For this two-dimensional problem, the h-conditioned Green's function was obtained via simulation and expressed in analytic form. It should be noted that the cumulative radial distribution found here is the same as that used previously by other researchers, and the analytic form of the conditional cumulative angular distribution comes from the two-dimensional Poisson kernel.

The ith estimate of the solution to the Poisson's equation is given by:

$$Z_i = \sum_{j=1}^{n_i} \int_{B(\mathbf{x_j}, r_j)} q(\mathbf{x})K(\mathbf{x}, \mathbf{z})d\mathbf{x} + f(X_{\tau_D^{\mathbf{x}}}^{\mathbf{x}}). \tag{7}$$

Here, n_i is the number of WOS steps needed for the ith Brownian trajectory to terminate in the ϵ-absorption layer, $\mathbf{x_j}$ is the center of the jth circle of radius r_j and $X_{\tau_D^{\mathbf{x}}}^{\mathbf{x}}$ is the first

passage location on the boundary, $\partial\Omega$. Instead of integrating the first term of Eq. 7, we can use the "one-point random estimation inside the sphere" method:

$$Z_i = \sum_{j=1}^{n_i} \frac{r_j^2}{4} E[q(Y_j)] + f(X_{\tau_D^{\mathbf{x}}}). \tag{8}$$

Here, Y_j is the sampling location inside the jth circle. At first, the radial position is selected according to the cumulative radial density and for the given radial position the angular position is selected according to the conditional cumulative angular distribution.

The error from the ϵ-absorption layer can be investigated empirically if we have enough trajectories so that the statistical sampling error is much smaller than the error from the ϵ-absorption layer. It turns out that the ϵ-layer error grows linearly in ϵ for small ϵ.

Recently, we developed a modified WOS algorithm for solving the linearized Poisson-Boltzmann equation in a domain Ω:

$$\Delta\psi(\mathbf{x}) = \kappa^2\psi(\mathbf{x}), \qquad \mathbf{x} \in \Omega, \tag{9}$$

$$\psi(\mathbf{x}) = \psi_0(\mathbf{x}), \qquad \mathbf{x} \in \partial\Omega. \tag{10}$$

Here, κ is called the inverse Debye length. We used a survival probability, which was obtained by reinterpreting a weight function in a previously modified WOS method. This survival probability enabled us to terminate some Brownian trajectories during WOS steps. This method can be combined with the method described in this paper to solve the Dirichlet boundary value problem for $\Delta\psi(\mathbf{x}) - \kappa^2\psi(\mathbf{x}) = -g(\mathbf{x})$. This will be the subject of a future study.

Also, it should be noted that the Feynman-Kac path-integral representation is general and the h-conditioned Green's function can be obtained for any geometry via simulation. This opens up the possibility of removing the ϵ-absorption layer in WOS methods.

Makoto Matsumoto [1]
Faculty of IHS
Kyoto University
Kyoto 606-8501, Japan
e-mail: `matumoto@math.h.kyoto-u.ac.jp`
`http://www.math.keio.ac.jp/matumoto/eindex.html`

Takuji Nishimura
Faculty of Science
Yamagata University
Yamagata 990-8560, Japan
e-mail: `nisimura@sci.kj.yamagata-u.ac.jp`

Title

A Non-empirical Test on the Weight of the Pseudorandom Number Generators Linear over $\mathbb{F}_2$

Abstract

There are a lot of pseudorandom number generators. Some are known to be defective, and some seem to be good.

GFSRs based on three-term relations are known to have statistical nonsymmetricity between 0 and 1, and to be rejected by χ^2-test on the goodness-of-fit to the binomial distribution, for more than thirty years.

However, these warnings were not loud enough to reach the users. These three-term GF-SRs were introduced in 1981 to the computational physics community by Kirkpatrick et.al. suggesting the recursion $x_j = x_{j-103} \oplus x_{j-250}$, and became fairly popular. In middle 80's, physicists began to find the failure of these generators in simulations of physical models, such as Ising models by Hoogland et.al., Ferrenberg et.al., and random walks by Grassberger. These physical models are simplified and proposed as tests of randomness by Vattulainen et.al., which we call physical tests here.

In these works some physicists' proposed two ways of improving GFSR: one is to increase the degree of the recurrence, and the other is to use five or more-term relations. These follow from an intuitive observation that few-term relations in a short range should lead to a deviation, and that increasing the number of terms or the range of the correlation will decrease the deviation. These improvements have been found to be effective in the physical tests.

However, it is not clear which degree is enough, or how many terms are enough for the required randomness. Five-term relations of degree 89 behave well for 10^6 samples, but are rejected for 10^8 samples by a random walk test conducted by Vattulainen et.al. A five-term relation of degree 1279 passed the test even for 10^9 samples. But... is this enough? The computational power of the machines is increasing rapidly. Will some defect of such a generator be revealed in the future? Or is it impossible for any future machine?

These physical tests are interesting in that they clearly exhibit the defects of random number generators in practical computational physics. However, they are not powerful in selecting good generators. Actually, these tests reject only (1) three-term GFSRs, (2) five-term GFSRs with small degree, and (3) linear congruential generators with poor spectral properties or short periods. All these generators are known to fail in some simple statistical tests. Also, these

---

physical tests cannot predict what will occur if we take the sample size larger and larger, exceeding the ability of present computers.

In this talk, we shall introduce a theoretical test on the distribution of 1s and 0s in the bits of the sequence, named *weight discrepancy test*. This is not an empirical test but a test on the full-period property of the generator, like the spectral test or the k-distribution test. It predicts with high precision the sample size for which the generator is rejected by the weight distribution test, which is a classical empirical test equivalent to a random-walk test. For example, the generator MT521 is shown to be quite safe with respect to this test, since it would require 10^{156} samples to reject its output, whereas the generator $R(11, 39, 95, 218)$ which passed all the physical tests done by Ziff et.al. is rejected if we take the sample size $> 600,000,000$ (and we confirmed this by empirical tests).

For simplicity, assume a random bit-sequence. For example, we may take the most significant bit of each of generated words, or take the most significant four bits of each of generated words and concatenate them.

Take m consecutive generated bits. The *weight* of this m-tuple is by definition the number of 1's among the m bits. Thus, it should conform to the binomial distribution if the sequence is uniformly and independently random. Group the set of weights into $\nu + 1$ categories, i.e., partition the set $\{0, 1, \ldots, m\}$ into $\nu + 1$ disjoint intervals

$$S_0 \cup S_1 \cup S_2 \cup \cdots \cup S_\nu = \{0, 1, 2, \ldots, m\}.$$

Let p_k ($k = 0, 1, \ldots, \nu$) be the probability that the weight falls into the k-th category S_k. Thus $p_k = \sum_{i \in S_k} \binom{m}{i} / 2^m$. We choose a grouping so that the probability p_k is not too small for every k (e.g., if the sample size is N, then Np_k is not less than, say, 10), as usual for χ^2-tests.

However, actually, the pseudorandom bit sequence is generated by a pseudo random number generator. We denote by q_k the probability that weight is k in the pseudorandom sequence, under the assumption that the initial seed is uniformly randomly selected.

The following value δ, called the χ^2-*discrepancy*, measures the distance between ideal p_k and realized q_k:

$$\delta := \sum_{k=0}^{m} (q_k - p_k)^2 / p_k.$$

The *weight discrepancy test* computes this χ^2-discrepancy δ.

This value δ is a good index of the deviation of the generator closely related to the χ^2-test. Let $\mathcal{X}_N$ be the result (i.e., the χ^2-value) of the χ^2-test for goodness-of-fit between the observed weights and the binomial distribution for N samples of m-tuples. This $\mathcal{X}_N$ is a random variable under the assumption that the initial seed is uniformly randomly selected, so we may consider its expectation $E(\mathcal{X}_N)$.

A simple computation tells that

$$|E(\mathcal{X}_N) - (\nu + N\delta)| \le \nu \max_{k=0,\ldots,\nu} \left| 1 - \frac{q_k}{p_k} \right|.$$

This shows that under the condition that q_k is close to p_k, which is always true for usable random number generators, $E(\mathcal{X}_N)$ is approximated by $\nu + N\delta$ regardlessly of each q_k.

Assume that δ is computed. By looking at the table of the χ^2-distribution with degree of freedom ν, we can compute N for which the sequence is rejected in average with significance level, say, 0.01, and thus we can estimate the dangerous sample size for which the pseudo random number shows deviation on the weight.

Computing δ seems to be NP-complete in general, but we use MacWilliams identity in the coding theory to obtain δ under some condition, and actually we obtained δ for various generators.

A smaller δ means a better fit to the theoretical distribution, so we can choose the best one from a set of generators, even if they pass the physical tests. In this regard, our test is similar to the spectral test and the k-distribution test. Moreover, our test gives an estimate for the dangerous/safe sample size, which is sometimes far beyond the power of the present computers.

We list δ for some common generators. We compare the results of experimental χ^2-tests with those expected from the value of δ. They show good accordance. We compute dangerous/safe sample size N for these generators, and show that some (Mersenne Twister, Combined Tausworthe,...) have astronomical N but others not. For example, Ziff's pentanomial GFSR $R(216, 337, 579, 1279)$ will be rejected for the sample size 1.7×10^{13}.

Wolfgang Mergenthaler
Bernhard Mauersberg
Jens Feller
Frankfurt Consulting Engineers
Kiefernweg 1
D-65439 Flörsheim
e-mail: WOLFMERG@aol.com
e-mail: Mauersberg@frankfurt-consulting.de
e-mail: Jens.Feller@t-online.de

William T. O'Grady Jr.
J. Stephen Ledford
Agilent Technologies
Integrated Workcell Business Team
12401 Research Blvd., Suite 100
Austin, TX 78759
e-mail: bill_ogrady@agilent.com
e-mail: steve_ledford@agilent.com

Leo J. Stuehler
Infineon Technologies AG
Quality Management / System Performance
St.Martin Str. 76
D-81541 München
e-mail: leo.stuehler@infineon.com

TITLE

Application of the Metropolis-Algorithm to Problems of Redudancy Elimination in Functional and Parametric Tests of Integrated Circuits

ABSTRACT

Integrated Circuits (IC's) are tested with respect to two different groups of tests. On the one hand there are functional tests which may either pass or fail, on the other hand there are parametric tests which usually result in a real number. Tests are costly procedures and in any case it is desirable to minimize testing effort, while, of course not loosing any information. It is obvious that reducing testing cost by dropping a non-optimized subset of tests will have an unpredictable impact on the outgoing quality of the population of IC's. Assuming, however, that tests are correlated among each other, one can hope that a certain subset of the full set of tests can be found such that, when eliminated, will not generate more than a given rate of defectives, usually in parts per million (ppm), while, on the other hand absorbing a maximal amount of testing time. A subset having this property with x ppm will be called x-redundant.

In the case of purely functional tests one usually finds a subset of defective IC's and a subset of intact IC's in every population. Any IC with at least one test failing is declared defective. In a production environment an IC is not tested beyond occurrence of the first defective test (First Failure Stop Strategy). In an experimental environment every function on each IC is tested (Full Test Strategy). In this paper a Full Test Strategy is assumed. Finding an x-redundant subset requires solving a combinatorial optimization problem. The type of problem is a set-covering problem. The objective function is the overall residual testing time, the dominating constraint consists in observing the upper bound of x ppm on the expected outgoing population quality and the decision variables are, of course, $(0-1)$ indicator variables on each test, where 0 stands for leaving the test in the set and 1 means dropping the test. The solution procedure is a Simulated Annealing approach, whereby the Metropolis algorithm is applied to each intermediate solution. Local search is controlled

by a set of operators acting on each intermediate redundant subset, making sure that the cardinality of a subset can approximately grow, remain constant and decrease with equal probabilities of $\frac{1}{3}$. The algorithm has been applied to real IC functional test data on various instances and revealed substantial redundancies, i.e. potential testing time reductions. The input data to the functional test reduction algorithm are a binary, rectangular matrix of IC tests, a vector of real numbers representing the testing times in milliseconds, the tolerated outgoing rate defective X and the yield of the IC population under consideration.

The case of parametric tests has so far been solved only theoretically. It is, however, of utmost industrial interest and therefore, intensive mathematical and algorithmic research is currently underway. The second part of this paper reports on pertinent results. The starting point is in observing that a finite set of tests can be modeled by a multivariate normally distributed random variable with a given covariance matrix and a vector of mean values. If this assumption is correct, the corresponding multivariate density can be formulated in closed form. Next, it is mandatory to note that even in the case of parametric tests, for each test an allowed interval is being defined such that an intact IC is one with each test result simultaneously in its proper, allowed region and a defective IC being one, with one or more test results being outside the allowed region. It is now straightforward to observe that the parametric case can be expressed as a functional case whereby the density of "1" or "0" entries depends on the definition of allowed regions on the tests. Of course, tighter tolerance limits will account for less "1"s and vice versa. But also, if that paradigm is unacceptable, the question may be asked, which of the test results will be in their respective allowed regions with a certain conditional probability of P greater than $1 - x \cdot 10^{-6}$, when the underlying tests are eliminated, given the remaining test results are observed to lie collectively in their allowed regions. Solving this question again yields a combinatorial optimization problem of the set covering type with the objective function being the residual testing cost for an IC as above, the constraint being given by the restriction on the conditional probability P and the decision variables defined as above. There are two severe performance obstacles to applying this procedure. Obstacle number 1 is the fact that, for each intermediate solution, a highly dimensional matrix must be numerically inverted. Obstacle number 2 originates from the fact that numerical integration of multiple integrals must be computed. While the latter problem can be overcome by using again a Monte Carlo method, the former constitutes an open question in numerical applied linear algebra: Is there any way to utilize the fact that a matrix inversion has been found, if this matrix is modified by subtracting a usually small number of lines and columns and by adding another usually small number of lines and columns ? Even if this question cannot be answered to the affirmative, the Metropolis algorithm can, when applied to this situation, contribute to substantial testing time reductions, since there is no need for the algorithm to have response times in the regions from seconds to minutes, but can, if necessary, run for two or more days, since the result, once known, may be valid for months. The input data are as above, except that the matrix of test results has now real number entries as opposed to "1"s and "0"s.

Experimental results will be shown.

Hozumi Morohosi [1]
National Graduate Institute for Policy Studies
2-2 Wakamatsu-cho, Shinjuku-ku
Tokyo 162-8677, Japan
e-mail: `morohosi@grips.ac.jp`

Masanori Fushimi [2]
Department of Mathematical Sciences
Nanzan University
27 Seirei-cho, Seto-shi
Aichi 489-0863, Japan
e-mail: `fushimi@ms.nanzan-u.ac.jp`

TITLE

Experimental Studies for the Error Estimation Methods of Quasi-Monte Carlo Integrations

ABSTRACT

The study of error estimation methods for quasi-Monte Carlo integrations attracts both theoretical and practical attentions currently. Several methods were proposed in recent years, and almost all of them are based on the idea of combination of Monte Carlo and quasi-Monte Carlo methods. They are often called "randomized quasi-Monte Carlo" methods, where the error of the numerical integration is estimated by the repetition of independent quasi-Monte Carlo samplings.

In [1] we presented some theoretical considerations on the error estimation methods, i.e. scrambling and randomly shifting methods, of quasi-Monte Carlo integrations and reported several numerical experimental results on Genz's test functions. Our experimental results show that both methods give reliable estimations of the errors.

In this talk we report some extensions to the results of our previous report [1]. Our extension is threefold: applying error estimation methods to real-world problems in financial engineering, increasing the dimension of the problems, and introducing various (t, s)-sequences in different bases into numerical experiments.

First we use the pricing problems of some financial derivatives, i.e., barrier options, Asian options, and look-back options are used to test the error estimation methods of QMC. These option pricing problems contain multidimensional integration problems (so-called path integrals) and they are one of the current main applications of QMC. Using those real-world problems we compare several error estimation methods in their reliability and precision of the estimated errors. Especially from the financial engineering viewpoint, above options raise the interest in their "path-dependent" properties. We examine how the different path-dependent properties of those options affect the efficiency of the error estimation methods.

Second we examine higher dimensional cases than in our previous report [1]. This extension follows naturally, because our new examples (option pricing problems) require several hundred dimensional integrals.

Third we compare several kinds of quasirandom sequences for each fixed dimension. In our previous report we examined two kinds of sequences, i.e. Sobol' sequence and Faure sequence,

---

for the same problems. In Niederreiter's general framework [2], Sobol' sequence is a (t,s)-sequence in base 2, and Faure sequence is a $(0,s)$-sequence in base p, where p is the smallest prime number greater than or equal to the dimension s. A natural question arises: how the selection of the base other than 2 or p affects the efficiency of the integration? We investigate this problem in terms of randomized QMC. We generate (t,s)-sequences in various bases following the Niederreiter's special construction [2], and then use a randomized version of them to obtain the error estimation in each example. Our analysis can be considered as an average case experimental analysis of the effect of base selection in (t,s)-sequence for numerical integrations.

References

[1] H. Morohosi and M. Fushimi: A practical approach to the error estimation of quasi-Monte Carlo integrations, *Monte Carlo and Quasi-Monte Carlo Methods 1998*, Springer, 2000.

[2] H. Niederreiter: *Random Number Generation and Quasi-Monte Carlo Methods*, SIAM, 1992.

Takuji Nishimura

Department of Mathematical Sciences
Yamagata University
Yamagata 990-8560, JAPAN
e-mail: `nisimura@sci.kj.yamagata-u.ac.jp`

Title

Defects of Commonly Used Pseudorandom Number Generators

Abstract

The rapid growth of the computational performance of the machines enables large-scale Monte Carlo simulations. This reveals hidden defects of some of commonly used generators, and underlines the necessity of high-quality and high-speed pseudorandom number generators.

LCGs with short period ($\simeq 2^{32}$) are classically known to be defective, because of their coarse lattice structure in high dimensions. Trinomial based GFSRs have a defect on the distribution of weights, which turns out to give an erroneous result in random walks and Ising model simulations, as was found out during the 1980–1990 period.

Since then, a lot of "improved" pseudorandom number generators have been proposed. We shall test these generators both theoretically and empirically, and make an extensive comparison both on the randomness and the speed.

These generators include: a very common lagged Fibonacci generator known as `random()` (introduced in 4.2BSD OS and widely spread in C-library in many versions of UNIX), trinomial-based GFSR proposed by Lewis and Payne in 1973, pentanomial-based GFSR proposed in many articles such as Ziff's (1998), twisted GFSR known as Mersenne Twister by Kurita, the author and Matsumoto in 1992, 1994 and 1998, a long period LCG like drand48, add-with-carry or subtract-with-borrow known as RCARRY introduced by Marsaglia and Zaman in 1991, its improvement RANLUX which discards large part of the output of RCARRY by Lüscher and James in 1994, and a similar improvement, called `ran_array`, of the lagged Fibonacci by Knuth in 1997, a rotated lagged-Fibonacci ranrot by Agner in 1999 and various combined generators such as a combined LCG `clcg4` by L'Ecuyer and Andres in 1997, a combined multiple recursive generator `combmrg2` by L'Ecuyer in 1999, a combined LFSR `lfsr113` by L'Ecuyer in 1999, a combined lagged-Fibonacci RANMAR by Marsaglia and Zaman in 1990.

A difficulty in such a comparison is that these improved generators pass all classical tests such as those in the Diehard battery by Marsaglia, although some of them show nonrandomness in large scale Monte Carlo simulations, i.e., if we take some larger sample size than those in Diehard test, then sometimes the generator shows a defect.

Consequently, our strategy is two-folded:

1. To find "natural" empirical tests which can detect the deviation of generators which pass the Diehard test but fail in some Monte Carlo simulation.

2. To find theoretical tests corresponding to the above tests, which estimate the dangerous sample size over which the empirical test will reject the generator, as well as the safe sample size.

(The idea to estimate the dangerous sample size is appeared in (1)(2)(3)(4).) These dangerous/safe sample sizes may be astronomical and then the generator would be empirically safe. For other generators, the size may be reachable by machines in the near future. Consequently, we can select "the best generators" in this sense.

There is a case where this is possible: if the generator is $\mathbb{F}_2$-linear and the test is the weight distribution test (this will be explained in the talk by Matsumoto). This test shows, for example, that pentanomial-based GFSR is far better than trinomial-based one, but still one can reject it by an experimental statistical test if the sample size is more than the dangerous sample size, which is often computable; e.g., it is $\simeq 10^{13}$ for the pentanomial with degree $= 1279$. Other such combinations are explained in (1)(2)(3)(4).

We shall generalize this idea. We fix a pseudorandom number generator G and assume that G generates a sequence of uniform pseudorandom numbers, in the interval I. If G is a real number generator, then I is usually $[0, 1)$, and if it is an integer generator, I is $\{0, 1, 2, \ldots, W - 1\}$ for a suitable integer W. Let S be the set of possible initial seeds of G. Assume that m consecutive outputs of G are used. Then, G can be simply regarded as a function $\Phi : S \to I^m$.

Now assume that the initial seed is uniformly randomly selected from the discrete set S. This makes S into a probability space, and Φ is a vector-valued random variable.

We fix some test function $f : I^m \to \mathbb{R}$. Under the null-hypothesis that the generated sequence is truly random, the distribution function of the random variable $f \circ \Phi$ is identical with that of f, where I^m is regarded as a probability space with the uniform measure on I^m.

In our previous talk, I is the two element field $\mathbb{F}_2$, and $f : \mathbb{F}_2^m \to \mathbb{R}$ is the weight function. In this talk we study the case where I is $[0, 1)$ and f is the sum over the m-tuples, i.e.,

$$f(x_1, \ldots, x_m) := x_1 + \cdots + x_m,$$

and measure the difference between the two random variables $f \circ \Phi$ and f, by χ^2-discrepancy. We apply the result to lagged Fibonacci and subtract-with-borrow generators.

We also point out specific defects of some widely used generators. For example, the original initialization scheme for random() in 4.2BSD has a fatal problem so that the sequence of the least significant bit of the outputs has only four possible patterns after each initialization, independently of the choice of the initial seeds. This defect is fixed in some OS including FreeBSD, but is left as it is in many OS like Solaris.

References

[1] P. L'Ecuyer and P. Hellekalek. Random number generators: selection criteria and testing. In P. Hellekalek and G. Larcher, editors, *Random and Quasi-Random Point Sets.* Lecture Notes in Statistics **138**, (1998), Springer, New York, 223–265.

[2] P. L'Ecuyer, R. Simard, and S. Wegenkittl. Sparse serial tests of uniformity for random number generators. GERAD report G-98-65, 1998.

[3] P. L'Ecuyer, J. F. Cordeau, and R. Simard. Close-point spatial tests and their application to random number generators. *Operations Research*, **48** (2000), 308–317.

[4] P. L'Ecuyer and R. Simard. On the performance of birthday spacing tests for certain families of random number generators. *Mathematics and Computers in Simulation*, **55** (2001), 131–137.

Gerald Paul
H. Eugene Stanley
Center for Polymer Studies and
Department of Physics
Boston University,
Boston, MA 02215
e-mail: `gerryp@bu.edu`
e-mail: `hes@argento.bu.edu`

Robert M. Ziff
Center for Theoretical Physics and
Department of Chemical Engineering
University of Michigan,
Ann Arbor, MI 48109-2136
e-mail: `rziff@engin.umich.edu`

Title

How To Build Very Large Percolation Clusters
with Very Little Computer Memory

Abstract

Percolation is a standard model for disordered systems (1; 2). In percolation systems, sites or bonds on a lattice are populated with probability p. The value of p at which infinite clusters are formed is known as the critical probability or percolation threshold p_c. Using Monte Carlo simulations to construct percolation clusters, one can estimate the percolation threshold and the exponents of quantities which obey power law scaling at the critical point. In order that finite size effects do not play a role, the lattice must be large enough such that the clusters that are grown do not reach the boundaries of the lattice. Because corrections-to-scaling decrease with the size of the clusters built, the larger the value of the clusters that can be built the more accurately we can estimate percolation thresholds and critical exponents. The limitations on the size to which the clusters can be grown have been the computer memory available to model the lattice and the computer processing power needed to build these clusters. The method of "data blocking" (3; 4) has helped ameliorate the need for large amounts of memory. In this method, the lattice is logically divided into blocks; memory for a block is not allocated until the lattice grows into that block. The data blocking method has been used recently to obtain precise estimates for the percolation threshold and associated exponents for bond and site percolation on a number of lattices (4; 5). Ultimately, however, although sufficient computer power is available to build larger clusters, the cluster size is limited by the amount of memory available. This becomes particularly true as the dimension of the lattice d increases since at criticality the cluster becomes less dense as d increases. To reach the same cluster mass we must have larger lattices.

In this paper we describe a method of constructing clusters which dramatically reduces the memory requirements needed to grow large clusters relative to previous methods. We use the Leath method(6) to construct clusters, but we keep track of which bonds are occupied and which sites have been visited by a method different from that traditionally used. Traditionally, this state information is stored in an array of size equal to the number of lattice sites. Vollmayr (7) eliminated the use of this array, storing status of visited sites in a data structure thus reducing memory requirements to grow a cluster of mass s to $O(s)$. We extend the approach of Ref. (7) further, reducing the memory required to $O(s^{\theta})$ where θ ranges from 0.4 for 2-dimensional lattices to 0.5 for 6- (or higher)-dimensional lattices. Our method involves:

172

(i) using a special random number generator.

(ii) using a hashing algorithm to access a table of visited sites.

(iii) using a new algorithm to build the cluster which limits the maximum number of sites for which we maintain state information to a number of the order of the number of sites in the largest chemical shell of the cluster being created.

Using the method described here, relative to computer processing power available today and in the foreseeable future, computer memory is no longer a constraint on building percolation clusters near the percolation threshold. The critical computer resource thus becomes solely processing power. For example, by extrapolating from our simulations, we find that with our method, with less than 10^8 bytes of memory, we could build a 5D cluster of 10^{12} sites, which(with traditional methods) would have required a lattice of 10^{17} sites. But the time to build a single trillion-site cluster would be about 2000 hours on current workstations. As processor speeds increase, our technique for reducing memory usage should allow critical exponents and constants to be determined with greater precision. Current techniques of growing clusters, including the one described in this paper, require computer processing resource of $O(s)$, where s is the size of the cluster grown.

Using our method of building large clusters, we estimate d_{min}, the exponent relating the shortest path ℓ to the Euclidean distance r, for hypercubic lattices in 4 and 5 dimensions. The study of critical properties in higher dimensions is important because one can use the results to test relations which are conjectured to hold in all dimensions (hyperscaling relations) and exponents which are believed to be the same in all dimensions (superuniversal exponents). The current best estimates of $d_{\min}$ for 4 and 5 dimensions, $1.63 \pm 0.03(8)$ and 1.8 (1), respectively, are of relatively low precision compared to the estimates available in 2 and 3 dimensions 1.1307 ± 0.0004 (9; 10; 11) and 1.374 ± 0.006 (12), respectively. We find $d_{\min} = 1.607 \pm 0.005$ (4D) and $d_{\min} = 1.812 \pm 0.006$ (5D). Thus our estimates of $d_{\min}$ are of higher accuracy than the existing ones and have accuracy comparable to that for the estimate of $d_{\min}$ in 3 dimensions.

References

[1] D. Stauffer and A. Aharony, *Introduction to Percolation Theory, 2nd Edition* (Taylor and Francis, London, 1994).

[2] A. Bunde and S. Havlin, eds., *Fractals and Disordered Systems, 2nd Edition* (Springer, New York, 1996).

[3] R. M. Ziff, P. T. Cummings, and G. Stell, J. Phys. A **17**, 3009 (1984).

[4] C. D. Lorenz and R. M. Ziff, Phys. Rev. E. **57**, 230 (1998).

[5] D. Stauffer and R. M. Ziff, Int. J. Mod. Phys. C **11**, 205 (2000).

[6] P. L. Leath, Phys. Rev. B **14**, 5046 (1976).

[7] H. Vollmayr, J. Stat. Phys. **74**, 919 (1994).

[8] P. Grassberger, J. Phys. A: Math. Gen. **19**, 1681 (1986).

[9] R. Pike and H. E. Stanley, J. Phys. A **14**, L169 (1981).

[10] H. J. Herrmann and H. E. Stanley, J. Phys. A **21**, L829 (1988).

[11] P. Grassberger, J. Phys. A: Math. Gen. **25**, 5475 (1992).

[12] P. Grassberger, J. Phys. A: Math. Gen. **25**, 5867 (1992).

Ad Ridder
Department of Econometrics
Vrije Universiteit Amsterdam
De Boelelaan 1105
1081 HV Amsterdam, Netherlands
e-mail: `aridder@feweb.vu.nl`
`http://www.feweb.vu.nl/medewerkers/aridder/`

TITLE

Efficient Simulation of a Rare Event in an Infinite Server Queue

ABSTRACT

Let be given an infinite server queue with Poisson arrivals and generally distributed service times. Suppose that at time 0 the system is empty. Then we consider the problem that the number of busy servers reaches level B for the first time in a given time interval $[T_1, T_2]$. The question is to determine its probability.

Infinite server queues are models popping up in inventory systems such as $(S-1, S)$, that is lot-for-lot ordering. Also, in telecommunication one uses infinite server queues to analyse system performance on call level. The problem described above is of interest in these applications since it concerns undesirable events: in inventory it means a stock-out, in telecommunication it means a call loss. By setting the target level B high, one tries to avoid these situations. Of course, because we deal with a stochastic system, there is always a — small — probability of occurence. So, we deal with a rare event.

This particular rare event problem is generally not solved. In case of exponential servers, the Laplace Transform of the first passage time can be expressed in a recurrence relation. Then, numerical inversion should give the probability. The disadvantage of this approach is that it is applicable for exponential servers only, and that the recursion runs in numerical problems since the recursion level equals the large B.

On the other hand, a simulation procedure is a general, easy-to-do, stable method which guarantees to give estimates of the probability. It is general in the sense that the computer program should be written in way that it can be executed for different service times, such as deterministic, Coxian, or Erlang. However, when dealing with a rare event, an accurate estimate requires long simulation times. In fact, it will take too long for estimating probabilities of the order 10^{-6} and smaller. In this paper we consider the method of importance sampling as a variance reduction technique, thus obtaining faster an accurate estimate.

To be more specific, since the target level B is high we denote $B = nb$, where b is fixed and n becomes large. In the same manner, the Poisson arrival rate is $\lambda = n\gamma$ for fixed γ. The factor n is a scaling factor with fluid limit implications. Finally, the service rate equals μ. We impose the requirement $\gamma/\mu < b$ for the following reason. Suppose that the service is exponentially distributed. Let $X_n(t)$ be the number of occupied servers in the n-system at time t. Then the fluid limit $X_n(t)/n \to \phi_m(t)$ holds ($n \to \infty$; for each t; in probability), where ϕ_m is a deterministic function, called the most likely behavior. Furthermore, $\phi_m(t) \to \gamma/\mu$

when $t \to \infty$. Thus, we see what happens for the fraction of occupied servers $X_n(t)/B$ when n and t becomes large: $X_n(t)/B = X_n(t)/(nb) \to \gamma/(\mu b) < 1$. This says that for large target levels the system size will stay below this level, eventually. Consequently, since ordinary Monte Carlo simulations generate sample paths of which almost all stay close to the most likely behavior ϕ_m, it takes a very long simulation before enough observations of the event have occurred.

In the paper we give the technical details of these matters. Also, applying large deviations, we find the most likely way how the rare event occurs. This is a deterministic function ϕ^* such that, conditionally on the event that the rare event occurs, $X_n(t)/n \to \phi^*(t)$ ($n \to \infty$; in probability). The idea of importance sampling is to change the underlying probability measure so that the function ϕ^* becomes the most likely behavior of the system. Thus, in the importance sampling simulations, the majority of generated sample paths will show the event of hitting the target level (in the target time interval $[T_1, T_2]!$). Applying large deviations, we prove that this method yields an asymptotically optimal estimator.

The new probability measure for the importance sampling simulations induces new interarrival time distributions and service time distributions which are exponentially tilted versions of the original distributions. However, since the optimal path to the target level (the function ϕ^*) is not a straight line, the tilting factor is updated continuously. In the implementation of the method, we update the factor only after each arrival or departure in the queueing process. The simulation results indicate that the estimator remains nearly asymptotically optimal.

As said above, the exact analysis of this approach is based on large deviations and can be done easily in case the service times are exponentially distributed. The optimal path to the target level is determined similarly as in the Erlang model (see Chapter 12 in [1], or [2]). For more general service time distributions this approach should be adopted, but, generally no exact results are known. However, in case of deterministic service times, when we observe the system state $X_n(t)$ at the times of departures of customers, we obtain a discrete-time Markov chain. This chain can be analysed, specifically, its most likely behavior, and the optimal path to high levels. Then, similarly as in the exponential case, importance sampling simulations are possible where the most likely behavior under the new measure mimics the optimal path. Since the service times are deterministic, only the distributions of the interarrival times are exponentailly tilted, again continuously. The main difference with the exponential case is that the tilting factors can not be given exact, but have to be calculated numerically.

References

[1] A. Shwartz, A. Weiss. *Large deviations for performance analysis, queues, communication, and computing.* Chapman & Hall, New York, 1995.
[2] M. Mandjes, A. Ridder. A large deviations approach to the transient of the Erlang loss model. *Performance Ananlysis* 43 (2001) 181-198.

Herbert Rief
Retired from the Joint Research Centre
of the Commission of the European Union
e-mail: `herbrief@tin.it`
oder: `herbert.rief@utanet.at`

Title

Light Propagation Modelling in Biological Tissue
by Advanced Monte Carlo Methods

Abstract

Laser techniques applied for diagnostic or therapeutic purposes require the detailed knowledge of the light path in tissue and diagnostic apparatus. In this paper algorithms are described which allow to analyse light propagation in complex 3D structures by advanced Monte Carlo techniques. The Monte Carlo program which has been developed in this context creates light trajectories as a function of time for wavelength dependent optical parameters. The photon propagation follows the classical scheme of neutral particle random walks allowing for absorption and different anisotropic scattering models (e.g.the Henyey-Greenstein phase function) as well as refraction and reflection at medium boundaries. Also an algorithm dealing with fluorescens has been incorporated. The geometry routine can handle multiple media bounded by quadratic surfaces used singly or in combinations.

The score functions are light flux, absorption and energy deposition in geometrical regions and photon transmission (temporal and spectral radiance) between specified geometrical regions.

As an unusual feature the program can optionally calculate derivatives and perturbations [1] of the photon density (at region boundaries) with respect to a density change in specified regions. This feature is based on *differential operator sampling* and aims at the calculation of small effects which can not be estimated by classical (analogue) Monte Carlo techniques. One of the essential quantities calculated is the sensitivity

$$S(R_{a,i,\gamma}) = \frac{\partial \psi(R_a, T_i)}{\psi(R_a, T_i)\partial \rho_\gamma}$$

where $\psi(R_a, T_i)$ is the area normalized number of photons crossing the surface which separates region a from region b, T_i the $i - th$ time interval ($T_i : t_i \leq t < t_{i+1}$) and ρ_γ the normalized material density of region γ.

Furthermore, the new program disposes of point detector algorithms which allow for the calculation of the radiance and its sensitivity at positions specified somewhere in the system. In particular the *track point estimator* (developed by the author et al.[2]) looks promising as it does not suffer of the r^{-2} singularity r being the distance between the collision point and the detector) typical for the *last collision estimator*. As shown by the same authors this algorithm has a $1/sin(x) \approx 1/x$ singularity and is particularly suited for problems in which strongly collimated particle beams are considered.

In some cases the uncertainty of estimates of particular interest can be decreased considerably replacing the analogue random walk procedure by the use of a forced collision scheme.

Prototypical examples explain the different features of the program including the analysis of a series of problems described in the literature and solved by Finite Element methods.

To illustrate the key feature of the program the following model has been considered: A tissue sample 10x5x5 cm (as shown in the figure) in which a spherical region ($r_\gamma = 0.5cm$) specified in the centre is analysed in terms of the sensitivities of the transmittance on its surface.
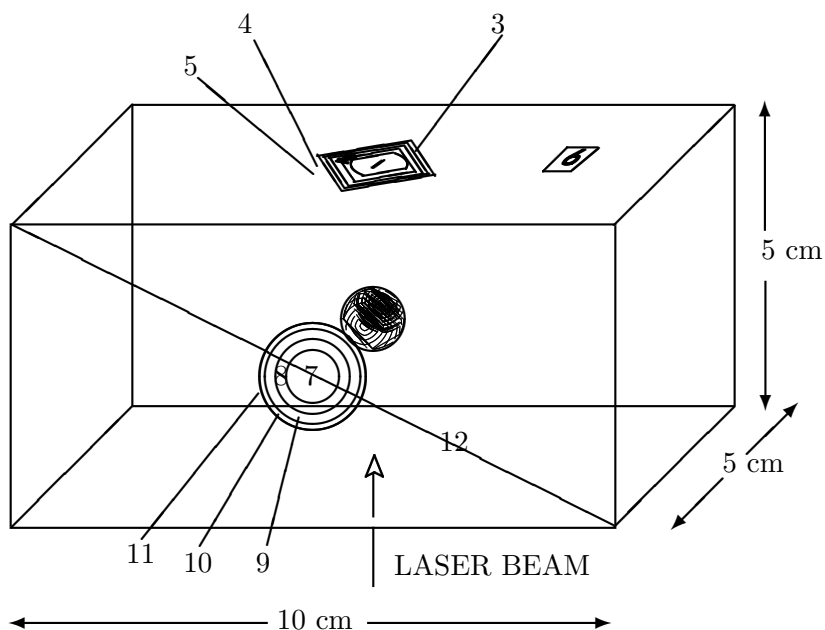
The sensitivities are calculated with respect to the density of the central spherical region for time bins and the numbered rings specified on top and side of the tissue sample. In this example the sensitivities provide a quantitative estimate for the fractional change of the photon density as a function of a fractional change of the density in the spherical region.

The estimates listed in both tables have been obtained following only 200.000 photon histories. Numerical values of the derivatives are listed in the following table:

Time Interval	transition to detector Rg:	1	2	3	4	5	6
0 - ∞	ψ	0.025	0.025	0.044	0.045	0.039	0.0089
	$\partial\psi/(\psi\partial\rho)$	- 0.181	- 0.270	- 0.209	- 0.167	- 0.134	0.048
0 - 2.3E-10	ψ	0.010	0.008	0.010	4.6E-3	1.1E-3	1.1E-6
	$\partial\psi/(\psi\partial\rho)$	- 0.63	- 0.523	- 0.59	- 0.634	- 0.77	0.078
2.3E-10 2.7E-10	ψ	0.014	0.015	0.033	0.036	0.037	6.1E-3
	$\partial\psi/(\psi\partial\rho)$	- 0.094	- 0.10	- 0.099	- 0.153	- 0.13	-0.021
2.7E-10 -1.E-9	ψ	1.6E-4	9.5E-5	4.8E-4	6.8E-4	4.8E-4	2.5E-3
	$\partial\psi/(\psi\partial\rho)$	0.045	0.14	0.047	-0.016	- 0.092	0.067

Transmission into Detector Regions on "Top" of Tissue Sample

Time dependence of laser-beam response functions;

Shortest possible path: 2.2365E-10.

The Radii for the Zylindrical Detector Regions are:

0.4472, 0.6325, 0.7746, 0.8944, 1.0 cm

In this table ψ is the number of photons (per cm^2 and per source photon) penetrating a specified surface-element. In the circular region 1 and time interval $0 - 2.3 \times 10^{-10}$ ψ would -for example- be 0.010. These are photons which mainly have to traverse the spherical region being subject of the change of density.

In the example above the sensitivity $\partial\psi/(\psi\partial\rho)$ says that a positive 1% density change in the 1cm radius sphere would lead to a 0.63% decrease of the number of photons penetrating surface element 1. (Notice the negative sign).

In the next table the same estimates are shown for the regions 7 to 11. They are on a plane perpendicular to the circular regions 1 to 6 and face directly the central sphere. Here one observes that the sensitivity has a positive value for the time interval $0 - 2.3 \times 10^{-10}$. This can be explained by the fact that increasing the number of scatterings in the central sphere the number of photons scattered to the "sides" is increased. As one would expect from qualitative considerations, a density increase favours the longer time intervals.

Time Interval	transition to detector Rg:	7	8	9	10	11
0 - 2.3E-10	transmission	0.0038	.0035	0.0070	0.0068	.0062
	sensitivity	0.015	0.037	0.018	0.028	0.021
2.3E-10- 2.7E-10	transmission	1.1E-4	1.1E-4	3.3E-4	3.2E-4	3.2E-4
	sensitivity	0.385	0.73	- 0.061	0.45	0.45
2.7E-10 - 1.E-9	transmission	1.4E-4	1.9E-4	3.2E-4	3.7E-4	3.2E-4
	sensitivity	0.220	- 0.0012	- 0.14	- 0.23	- 0.028

Detector Responses at the "side" of the Tissue Sample
Time dependence of laser-beam response functions;
Radii for the zylindrical detector regions:
0.4472, 0.6325, 0.7746, 0.8944, 1.0 cm

In both tables it can be seen that the sensitivity is strongly dependent on the time interval.

So far in the case of Monte Carlo calculations only large parameter changes could be analysed since the variance of the difference of independent simulation estimates are larger than the differential effects one is looking for.

References:

1. Rief H., "Stochastic Perturbation Analysis Applied to Neutral Particle Transport" in Advances in Nuclear Science and Technology, Vol. 23 (1996)

2. Rief H., Dubi A. and Elperin T., "Track length Estimation Applied to Point Detectors", Nucl. Sci. and Engi. 87, 59-71 (1984)

3. Doyle J.P. and Rief H.," Photon Transport in 3D Structures Treated by Random Walk Techniques: Monte Carlo Benchmark of Ocean Colour Simulations" Mathematics and Computers in Simulation, 47 (1998) 215-241; IMACS/Elsevier Science B.V.

Marco Saraniti
Jinsong Tang
Department of Electrical and
Computer Engineering
Illinois Institute of Technology
3301 South Dearborn,
60616 Chicago, IL. (U.S.A.)
e-mail: `saraniti@iit.edu`

Stephen M. Goodnick
Shela J. Wigger
Electrical Engineering Department
Arizona State University
Tempe, AZ. (U.S.A.)

Numerical Challenges in Particle-Based Approaches for the Simulation of Semiconductor Devices [1]

ABSTRACT

Introduction. The aim of this paper is to review and discuss the most challenging aspects of the particle-based methods for simulation of charge transport in semiconductor devices. Since the early theoretical works on the Monte Carlo (MC) method applied to device simulation (10; 12; 7), and several successive reference texts addressing both the physics (6) and the numerical aspects (5) of the MC method, the basic algorithmic approaches have been modified to exploit the continuous improvements of both hardware and software tools. Typical examples of the algorithmic evolution are the adoption of the full band representation of the electronic structure (3), the so-called cellular automaton (CA) (9; 13), and the simulation of increasingly complex 3D structures (15; 16). This paper will address some of the most significant problems which are still considered open in spite of the recent technological and scientific progresses.

Physics: the full band approach. Initially developed by K. Hess and co-workers (14), the full band MC method has been fully implemented by Fischetti and Laux in 1988 (3). Allowing to correctly represent the carrier dynamics in the Brillouin Zone (BZ) of momentum space, the full band approach has undeniable advantages over less accurate analytical representations of the electronic structure. However, the numerical representation of the momentum space requires a more complex algorithmic approach, and increases the need of computational resources. In particular, it seems clear that an in-homogeneously spaced grid, either rectangular (13) or tetrahedral (2) is required to correctly model the low-field behavior of semiconductors. This paper will show that this kind of "smart" grids also allow an accurate reproduction of experimental data on ultra-fast transient response of semiconductors such as GaAs and InP (11).

Furthermore, the inclusion of anisotropic scattering rates in the full band MC framework is an improvement that is highly costly in terms of computational resources.

Scattering selection schemes: Monte Carlo and cellular automaton. The availability of computers equipped with large amount of fast memory (RAM) triggered a noticeable

---

modification of the basic scattering algorithm in the MC programs. In particular, within the full-band MC framework, the inversion of the energy-momentum dispersion relation is required after the occurrence of each scattering. In facts, the entire discretized BZ has to be scanned to find all the energy-conserving sites (cells). Even a smart searching algorithm based on a three-dimensional recursive binary tree, and limited to the IW of the BZ, takes a relatively long time to find the candidate sites. This effect is more evident at high fields, when scattering events are more frequent. Implementations of efficient algorithms to reduce time of this final state selection process in full band simulators have been reported based on simplexes (1) and rejection techniques (8). Another approach which is current under investigation is the so-called cellular automaton, described below.

The idea of storing the transition probability from any initial state to all possible final states has been firstly implemented in the energy domain by Vogl and co-workers (9), and has been recently extended to the full band representation by Saraniti and Goodnick (13). This approach dramatically reduced the time required to process scattering events, allowing for shorter total simulation times. The resulting method has been called (mostly for historical reasons) "cellular automaton", because of some resemblance of the early implementations with the approach used to model the dynamics of complex systems. (17).

The algorithmic evolution of the full band CA, and of its hybrid variant (13), where the traditional Monte Carlo approach is used in sub-regions of BZ where less scattering occur, will be the main topic of the present contribution.

The speed-up obtained by the CA algorithm is impressive (up to 50 times), and the possibility of cost-less inclusion of anisotropy in the CA scattering tables makes the method definitely attractive. However, energy conservation issues are arising, due to the coarseness of the momentum discretization grid. Several optimization techniques will be presented other than the above mentioned hybrid approach to reduce the required memory and increase the energy resolution.

Numerics: particle tracking. A crucial requirement of particle-based approaches (both CA and MC) is the capability of efficiently track the dynamics of the components in the phase-space. Given the high number of carriers required to model a realistic device, the particle tracking technique is crucial for the performance of both the position- and the momentum-space tracking algorithm. It is evident that a trade-off exists between the high flexibility of tetrahedral (or triangular) grids and the difficulty of tracking particle trajectories moving from cell to cell. While the choice of the authors is to use rectangular grids both in position and momentum-space, several other successful approaches exist that make use of tetrahedral grids (2). No satisfactorily detailed comparison has been made, to the best of the authors' knowledge, of simulators based on differently structured grids, and the need of a final word on that issue will be stressed as well.

Numerics: parallel computing. The idea of using special parallel hardware to speed up the execution of particle-based simulators is an old one. The partially local nature of some of the carrier interactions makes natural the parallel computing choice. Recent interesting developments resulted in the the fact that a "special parallel hardware" is not required anymore. In facts, cheap and efficient interprocess communication software (4) made possible to use groups of conventionally networked workstations ("computer clusters") as an individual

parallel platform. A discussion will be carried out about the parallel versions of the particle-based algorithms and parallel performance results will be presented. Optimal architectures for the problems of interest will be discussed as well.

References

[1] J. Bude and R.K. Smith. Phase-space simplex Monte Carlo for semiconductor transport. *Semiconductor Science and Technology*, 9:840–843, 1994.

[2] B. Fischer and K.R. Hofmann. A full-band Monte Carlo model for the temperature dependence of electron and hole transport in silicon. *Applied Physics Letters*, 76(9):583–585, January 2000.

[3] M.V. Fischetti and S.E. Laux. Monte Carlo analysis of electron transport in small semiconductor devices including band-structure and space-charge effects. *Physical Review B*, 38(14):9721–9745, November 1988.

[4] R. Hempel. The MPI standard for message passing. In Wolfgang Gentzsch and Uwe Harms, editors, *High-Performance Computing and Networking*, number 797 in Lecture Notes in Computer Science, pages 247–252, Berlin, April 1994. Springer–Verlag.

[5] R.W. Hockney and J.W. Eastwood. *Computer Simulation Using Particles*. Adam Hilger, Bristol, 1988.

[6] C. Jacoboni and P. Lugli. *The Monte Carlo Method for Semiconductor Device Equations*. Springer–Verlag, Wien, NewYork, 1989.

[7] C. Jacoboni and L. Reggiani. The Monte Carlo method for solution of charge transport in semiconductors with applications to covalent materials. *Reviews of Modern Physics*, 55(3):645–705, July 1983.

[8] C. Jungemann, S. Keith, M. Bartels, and B. Meinerzhagen. Efficient full-band Monte Carlo simulation of Silicon devices. *IEICE Transaction on Electronics*, E82-C(6):870–879, June 1999.

[9] K. Kometer, G. Zandler, and P. Vogl. Lattice–gas cellular–automaton method for semiclassical transport in semiconductors. *Physical Review B*, 46(3):1382–1394, July 1992.

[10] T. Kurosawa. Monte Carlo calculation of hot electron problems. In *Proceedings of the International Conference on the Physics of Semiconductors*, volume 21, Supplement to the Journal of the Physical Society of Japan, pages 424–426, Kyoto, 1966.

[11] A. Leitenstorfer, S. Hunsche, J. Shah, M.C. Nuss, and W.H. Knox. Ultrafast high-field transport in semicnductors. *Physica B*, 272:348–352, 1999.

[12] A. Phillips and P.J. Price. Monte Carlo calculations on hot electron energy tails. *Applied Physics Letters*, 30(10):528–530, May 1977.

[13] M. Saraniti and S.M. Goodnick. Hybrid full-band Cellular Automaton/Monte Carlo approach for fast simulation of semiconductor devices. *IEEE Transactions on Electron Devices*, October 2000. (Accepted for Publication).

[14] H. Shichijo and K. Hess. Band-structure-dependent transport and impact ionization in GaAs. *Physical Review B*, 23(8):4197–4207, Apr 1981.

[15] S.J. Wigger. Three dimensional multigrid poisson solver for use in semiconductor device modeling. Master's thesis, Arizona State University, Tempe, AZ, Aug 1998.

[16] S.J. Wigger, M.Saraniti, and S.M. Goodnick. Three-dimensional Multi-grid Poisson solver for modeling semiconductor devices. In *Proceedings of Second International Conference on Modeling and Simulation of Microsystems, MSM99*, pages 415–418, Puerto Rico (PR), April 1999.

[17] S. Wolfram. Cellular automata as models of complexity. *Nature*, 311:419–424, October 1984.

Mateu Sbert
Institut d'Informatica i Aplicacions
Universitat de Girona
Lluis Santalo, s/n
E-17071 Girona, Spain
e-mail: `mateu@ima.udg.es`

TITLE

Optimal Gathering Random Walk Absorption Probabilities for Radiosity in Scenes with Large Area Sources

ABSTRACT

Optimal absorption probabilities for gathering random walk (3) were studied in (1) in the radiosity setting and (2) in the general global illumination setting. In (1) we showed that if we neglect the second order term in the reflected radiosity b_i appearing in the expression for the variance, the optimal absorption probabilities θ_i were equal to the reflectivities R_i. We will study here the general case, this is, the term b_i^2 can not be neglected.

The expression for the efficiency of the gathering random walk is (1)

$$\left(\frac{f}{1-\left(\frac{R_{ave}^2}{\theta_{ave}}\right)} - k \times f \right) \times \left(\frac{1}{1-\theta_{ave}} \right)$$

where the first term is the expected value of the Mean Square Error, the second term is the average length of a path and f and k are scene dependent parameters (k depending on the b_i^2 values). We have used (and will use throughout this paper) the approximation that $R_{ave}^2 = (R_{ave})^2 \approx (R^2)_{ave}$. This quantity has as optimal values:

$$\theta_{ave1} = \frac{kR_{ave}^2 - R_{ave}\sqrt{1-k+kR_{ave}^2}}{-1+k}$$

and

$$\theta_{ave2} = \frac{kR_{ave}^2 + R_{ave}\sqrt{1-k+kR_{ave}^2}}{-1+k}$$

From the discriminant we have that $k \leq \frac{1}{1-R_{ave}^2}$. Also from the denominator $k \neq 1$. The quantity k is also positive, and equal to

$$k = \frac{\frac{\sum_i A_i b_i^2}{A_T}}{\frac{\sum_s (E_s + 2b_s)\Phi_s \times R_{ave}^2}{A_T}}$$

where A, E ,Φ are area, emissivity and power, respectively, subindex s indexes the sources and A_T is the total area. Thus $0 < k \leq \frac{1}{1-R_{ave}^2}$ and $k \neq 1$. The case $k = 0$ was the one considered in the (1), this is, b_i^2 quantities neglected, and $\theta_{ave1} = R_{ave}$. Our interest here is to study the general case $k > 0$. After some approximations similar to the ones used in (1), we obtain

$$k = \frac{1}{(1-R_{ave})\left((1-R_{ave})A_T \frac{\sum_s E_s \Phi_s}{\Phi_T^2} + 2\frac{\sum_s R_s \Phi_s}{\Phi_T}\right)}$$

where Φ_T is the total power. We see inmediately that $k = 1$, the discontinuity case in the θ_{ave} solutions, only can happen when $R_{ave} = 0$ (in which case also all $R_s = 0$), which is a consistent result. Also, considering the particular case of equal area and power for all sources,

$$k = \frac{1}{(1-R_{ave})((1-R_{ave})\frac{A_T}{A_S}+2R_{s_{ave}})}$$

where we see the influence on the result of the fraction of area covered by the sources $\frac{A_S}{A_T}$. In the limiting case where $A_T = A_S$ it is clear that $R_{S_{ave}} = R_{ave}$ and k becomes

$$k = \frac{1}{(1-R_{ave})((1-R_{ave})+2R_{ave})} = \frac{1}{1-R_{ave}^2}$$

It is easy to see that for this value $\theta_{ave1} = 1$. Thus for a uniform source covering all the scene the optimal (limiting) case is when the path always survives. We see also that for $\frac{A_S}{A_T} << 1$ then $k \approx 0$, which means that for small area sources the result in (1) is a very good approximation. Now our interest will be in finding the θ_{ave} optimal value in the in between cases, relating it to R_{ave}, and from this relation to be able to deduce a relationship between R_i and θ_i values for all i. Although the big area source case might look at first sight uninteresting, most radiosity problems can be converted into it by using the so called first shot (4)(5), this is, expanding first the illumination from the sources and converting the receiving patches into new sources with emissivity equal to the reflected direct illumination.

References

[1] Mateu Sbert, Optimal absorption probabilities for Random Walk Radiosity, Graphical Models **62**, 56-70 (2000).

[2] Gyorgy Antal and Laszlo Szirmay-Kalos, Finding Good Termination Probability for Random-walks, In Spring Conference on Computer Graphics'2000 (SCCG'2000), pp.205-211, 2000.

[3] Philippe Bekaert. Hierarchical and Stochastic Algorithms for Radiosity. PhD dissertation, KU Leuven, 1999.

[4] Francesc Castro, Roel Martinez and Mateu Sbert, Quasi-Monte Carlo and extended first shot improvements to the multi-path method. In Spring Conference on Computer Graphics'98 (SCCG'98), pp. 91-102, 1998.

[5] Laszlo Szirmay-Kalos, Mateu Sbert, Roel Martinez and Robert Tobler, Hardware First-Shot for Non-Diffuse Global Illumination. In Spring Conference on Computer Graphics'2000 (SCCG'2000), pp.197-204, 2000.

Christoph Schlier [1]
Fakultät für Physik
Universität Freiburg
Hermann-Herderstr. 34
D-79 104 Freiburg, Germany
e-mail: `schlier@uni-freiburg.de`
`http://www.physik.uni-freiburg.de`

TITLE

A Practitioner's View on QMC Integration

ABSTRACT

This paper is mostly empirical. We report on extensive tests of QMC integration in dimensions 3, 6, 12, and 24, employing different test integrands, different low discrepancy sequences, and large ($>10^{11}$) numbers of trials. In contrast to the "folklore" about QMC integration, we find that neither the asymptotic discrepancy formulas for the sequences nor the variations of the integrands are a useful means to estimate the integration errors in practical cases. Instead, it has proven useful to repeat the integration several (e.g. 10) times with consecutive pieces of QR points from a single sequence, and to use mean and standard deviation of these repetitions to estimate the integral and its error. These errors are, of course, not worst case errors, nor exact statistical average errors. But, as is well known, the asymptotic worst case error formulas from the literature are unrealistic large (factors between 10^5 and 10^{15} in our examples). Still they are cited, even if they are useless in practice.

In order to shed some light on these differences we also computed numerical approximations to the true discrepancies $D^*(N)$ for N up to 10^9. The values of D^*, too, follow power laws, and in the logarithmic scale are about half-way between the asymptotic D^* and the realistic errors divided by the variation of the integrand. If one accepts extrapolation to much larger numbers, one must conclude that the true and the asymptotic discrepancies D^* do not meet before N = 10^{50} or more.

The full paper will show in figures and tables the following details:
1) The practical integration error is never found to behave as $\log(N)^s/N$ as the asymptotic worst case predicts, but always (within some fluctuation, of course) as a power law. The power is $-1/2$ - $1/2s$ for characteristic functions, and between -1 and -1/2 for continuous functions. In the latter case it depends on the integrand, and approaches -1/2 for large dimensions. The absolute positions of the error in the plots is determined by the rule that a linear extrapolation of the log-log plot to N = 1 meets approximately the pseudo-random value sqrt(var(f)).
2) We also computed the variation of several of the test functions. For most of them the ratio of the variation over the square root of the variance increases exponentially with dimension. Therefore, the variance, not the variation plays the decisive role for the size of the average error.

---

3) We compared the errors from integration with Halton sequences using different sets of primes, and Niedereiter (t,s)-sequences with different bases. We never found the large error ratios predicted by the pre-factors of the asymptotic $\log(N)^s/N$ law, but rather modest spreads. Such modest differences are also found for the true discrepancies. Especially, Halton sequences using the lowest s primes, and Niederreiter sequences to base 2 have generally comparable errors, and Niederreiter sequences with base 2 are often better than those with the so called "optimal" base.

4) From the comparison of the mean errors and their standard deviation we conclude that the distribution of the errors of our repeated integrations is somewhat broader than a Gaussian, showing an excess which increases with dimension.

5) We also tried several simple randomization schemes for the repetitions in our method. Their influence was, however, small, once the number of trials exceeded 10^4. Note that randomization schemes like Owen's, in which the permutations of the sequences must be stored in memory, are not feasible for large numbers of trials because of lack of computer memory.

It is obvious, that our results are of limited generality. The maximum number of trials was, of course, restricted by the available computing resources. But we feel that the log-log plots of the errors and of the discrepancies are linear enough, to allow extrapolation to at least 10^{16} trials, which will, perhaps, be available for integration in 2015. Moreover, there are certainly function classes, which behave differently from our test functions. Indeed, we hope that more exact formulas for the average errors for certain function classes will be derived, which can also be implemented with limited expense by the common user. Nevertheless, we feel, that the tool of QMC integration is so advantageous, that it should be used even before its limits are fully known.

Rudolf Schürer [1]
Department of Scientific Computing
University of Salzburg
Hellbrunnerstr. 34
A-5020 Salzburg, Austria
e-mail: `rudolf.schuerer@sbg.ac.at`
`http://www.cosy.sbg.ac.at/~rschuer/`

TITLE

A Comparison between Quasi-Monte Carlo and Cubature Rule Based Methods for Solving High-Dimensional Integration Problems

ABSTRACT

The problem of estimating the integral of a function $f : C_s \to \mathbb{R}$ over a hyper-rectangular region $C_s \subset \mathbb{R}^s$ is considered. Solving this problem in high dimensions is usually considered a domain of Monte Carlo and quasi-Monte Carlo methods, because, compared to most alternatives, the theoretical power of these techniques degrades little with increasing dimension.

In this work, quasi-Monte Carlo techniques based on (t, s)-sequences as well as Monte Carlo algorithms are compared to integration routines based on common interpolatory cubature rules, which are usuallay not used in dimensions beyond about $s = 10$. These algorithms can be built in an adaptive as well as a non-adaptive fashion, and can be based on a wide range of different cubature rules with highly varying properties.

For these empirical tests, which are carried out for dimensions up to $s = 100$, a number of different test integrands with different attributes are used, including all integrands from Genz's test function package.

After introducing all evaluated routines, this work focuses on pointing out the strength and weakness of each algorithm. Special care is taken to investigate which integration routine is most suitable for a given integrand functions in a given dimensions, and to determine the reason for this behavior.

For certain integrands, it turns out that cubature rule based algorithms can provide more accurate results than quasi-Monte Carlo routines for dimensions up to $s = 100$.

I.M.Sobol'
D.I.Asotsky
Institute for Mathematical Modelling
4a Miusskaya Square
Moscow 125047, Russia
e-mail: `hq@imamod.ru`

TITLE

One More Experiment
on Estimating High-Dimensional Integrals
by Quasi-Monte Carlo Methods

ABSTRACT

The mean value formula for estimating high dimensional integrals is considered and its approximation error

$$\delta_N[f] = \frac{1}{N}\sum_{k=0}^{N-1} f\left(x^{(k)}\right) - \int_0^1 ... \int_0^1 f(x)\,dx$$

is studied. Here $x=(x_1,..., x_n)$. In the crude Monte Carlo method (MC), the nodes $x^{(k)}$ are independent values of the random point ξ uniformly distributed in the unit hypercube. If the variance $Df(\xi)$ is finite, the probable error of MC is $r_N = 0.6745\sqrt{Df(\xi)/N}$; it decreases as $1/\sqrt{N}$. For quasi-Monte Carlo estimates (QMC) the nodes $x^{(k)}$ are nonrandom points of a sequence called quasi-random. Sometimes the QMC convergence rate is $\delta_N = O(1/N)$. The most important problems where QMC is more efficient than MC include integrands $f(x)$ whose dependence on x_i decreases as the number i is increased. However, the situation is more obscure if all the variables $x_1,...,x_n$ are equally important. On one hand, simple examples demonstrate the advantage of QMC at relatively small dimensions only (most authors suggest $n \leq 12 \div 15$). On the other hand, problems from financial mathematics are known where QMC outplays MC at $n=360$. Recently, Prof. H. Rabitz has suggested that quite often in mathematical models the low order interactions of input variables have the main impact upon the output. In the ANOVA-representation of such models

$$f(x) = f_0 + \sum_i f_i(x_i) + \sum_{i<j} f_{ij}(x_i, x_j) + ... + f_{12...n}(x_1, x_2, ..., x_n)$$

the main terms are the low order ones. Clearly, QMC integration of such functions will be rather efficient even when n is large and the variables are equally important.

2. The present experiment. We have selected a set of test functions depending on a parameter c, $0 < c \leq 1$,

$$f(x) = \prod_{i=1}^n \left[1 + c\left(x_i - \frac{1}{2}\right)\right].$$

The case $c=1$ has been considered earlier but only for dimensions $n \leq 50$. In our experiment $n \leq 300$. For $x^{(k)}$, points of LP_τ-sequences (that are often called Sobol sequences) were selected. We have used the "superfast" program from [1]. The number of nodes $N \leq 2^{28}$.

3. Small c. An asymptotic formula was proved: for arbitrary n and N

$$\delta_N [f] = -\frac{nc}{2N} + O\left(c^2\right).$$

Then for several fixed values of N, level lines $|\delta_N| = const$ were computed. For moderate nc we got hyperbolas $nc = 2N |\delta_N|$. In cases where $N |\delta_N|$ converge as N increases, the limit is likely to be $nc/2$.

4. Large N. Applying the Koksma-Hlawka inequality one can prove that $\sqrt{N}\delta_N [f] \to 0$ as $N \to \infty$. Therefore $\delta_N/r_N \to 0$ and QMC always outplays MC at $N \to \infty$. However in practice, the amount of points N is restricted, and the relations between δ_N and r_N are different. Let $N \leq 2^{25}$. Then at $nc < 15$ errors $|\delta_N|$ behave like $1/N$; at $15 \leq nc < 35$ the $|\delta_N|$ decrease faster than r_N, while at $35 \leq nc < 60$ they are of the same order of magnitude. Finally, at $nc > 60$ the $|\delta_N|$ are much larger than r_N, and MC becomes more expedient than QMC.

5. Examples.

N	$nc=6$ $n=24,c=0.25$ $N\,|\delta_N|$	$nc=12$ $n=120,c=0.1$ $N\,|\delta_N|$	$nc=24$ $n=96,c=0.25$ $\sqrt{N}\,|\delta_N|$	$nc=50$ $n=200,c=0.25$ $\sqrt{N}\,|\delta_N|$	$nc=150$ $n=150,c=1$ $\sqrt{N}\,|\delta_N|$
2^{16}	1.43	17.8	0.20	8.90	14200
2^{18}	2.61	15.3	0.07	4.65	7210
2^{20}	1.52	25.5	0.11	0.94	3560
2^{22}	3.04	28.2	0.03	0.22	1740
2^{24}	2.59	3.4	0.007	0.28	1020
2^{26}	2.78	8.8	0.015	0.58	292
2^{28}	2.87	18.7	0.007	0.12	929
	$nc/2 = 3.0$	$nc/2 = 6.0$	$\sqrt{N}r_N = 0.42$	$\sqrt{N}r_N = 0.70$	$\sqrt{N}r_N = 8.4$

6. Conclusion. One should be careful with QMC if there are very many important variables.

Reference [1] I.M.Sobol', V.I.Turchaninov, Yu.L.Levitan, B.V.Shukhman. Quasirandom Sequence Generators. Keldysh Inst. Appl. Maths., Moscow, 1992, 22p.

Tatiana M. Tovstik
Irina A. Vinogradova
Valentina A. Myshenskaya
Department of Mathematics and Mechanics
St.Petersburg University
Bibliotechnaya sq. 2
198904, Petrodvorets, St.Petersburg, Russia
e-mail: `Peter.Tovstik@pobox.spbu.ru`
e-mail: `Vinirka@yahoo.ru`

Simulation of the
Isotropic Homogeneous Random Field in R_3

ABSTRACT

The expansion in spherical functions of a homogeneous isotropic field in R_3 is an infinite sum of the stochastic integrals with infinite limits. For the given in the root-mean-square sense exactness ε the approximate model with the finite limits is constructed. This model is used for the field simulation.

Let $v = (x, y, z) \, \epsilon \, R_3$ and (r, φ, θ) be the spherical co-ordinates of the point v. Then the isotropic field $\eta(v) = \eta(r, \varphi, \theta)$ with $\mathbf{E}\eta(v) = 0$, $\mathbf{D}\eta(v) = 1$ has the spectral representation [1]

$$\eta(v) = \eta(r, \varphi, \theta) = \sum_{m=0}^{\infty} \sum_{k=0}^{m} A_m^k P_m^k(\cos\theta) \times$$

$$\times \left[\cos(k\varphi) \int_0^{\infty} j_m(\lambda r) dz_m^{k1}(\lambda) + \sin(k\varphi) \int_0^{\infty} j_m(\lambda r) dz_m^{k2}(\lambda) \right], \tag{1}$$

$$A_m^0 = [2m+1]^{1/2}, \quad A_m^k = \left[2\frac{(2m+1)(m-k)!}{(m+k)!} \right]^{1/2}, \ k > 0.$$

Here the following designations are used: $P_m^k(\lambda)$ are the attached Legendre polynomials, $j_m(\lambda)$ are the Bessel spherical functions of the 1-st kind, $z_m^{k1}(\lambda)$, $z_n^{l2}(\lambda)$ are the independent processes with the orthogonal increments and such that

$$\mathbf{E}dz_m^{k1}(\lambda) = \mathbf{E}dz_n^{l2}(\lambda) = 0, \tag{2}$$

$$\mathbf{E}dz_m^{ls}(\lambda)dz_n^{kt}(\lambda) = \delta_m^n \delta_l^k \delta_s^t f(\lambda)d\lambda. \tag{3}$$

In relations (3) the Kronecker symbol δ_j^k is used, and $f(\lambda)$ is the radial spectral density. The correlation between the field points $v_j = (x_j, y_j, z_j)$, $j = 1, 2$, is equal

$$R(\rho) = \mathbf{E}\eta(v_1)\eta(v_2), \quad \rho^2 = (x_1 - x_2)^2 + (y_1 - y_2)^2 + (z_1 - z_2)^2, \tag{4}$$

and

$$R(\rho) = \int_0^\infty \frac{\sin(\lambda\rho)}{\lambda\rho} f(\lambda)d\lambda.$$

We choose value $\varepsilon > 0$ and find three approximations $\eta_A(v)$, $\eta_{A,N}(v)$ and $\eta_{A,M,N}(v)$ of the field $\eta(v)$ which successively differ from $\eta(v)$ and from the each other no larger than by $\varepsilon/3$.

We get the field $\eta_A(v)$ from representation (1) by changing the integral limits $(0, \infty)$ to $(0, A)$. As $R(0) = \int_0^\infty f(\lambda)d\lambda = 1$, then the value A such that $\int_A^\infty f(\lambda)d\lambda < \varepsilon/3$ may be found. For this A

$$\mathbf{E}|\eta(v) - \eta_A(v)|^2 = \int_A^\infty f(\lambda)d\lambda < \varepsilon/3. \tag{5}$$

We divide the interval $(0, A)$ in N equal parts $(\lambda_n, \lambda_{n+1})$, $n = 0, 1, \ldots, N-1$, of the length $\Delta = A/N$, $\lambda_n = n\Delta$, and each of the integrals in the field $\eta_A(v)$ representation (see (1)) we rewrite as a sum of N integrals. For example, $\int_0^A j_m(\lambda r)dz_m^{k1}(\lambda) = \sum_{n=0}^{N-1} \int_{\lambda_n}^{\lambda_{n+1}} j_m(\lambda r)dz_m^{k1}(\lambda)$.

Then we introduce the field

$$\eta_{A,N,M}(v) = \sum_{m=0}^{M} \sum_{k=0}^{m} A_m^k P_m^k(\cos\theta) \left[\cos(k\varphi) \sum_{n=0}^{N-1} j_m(\tilde\lambda_n r) \int_{\lambda_n}^{\lambda_{n+1}} dz_m^{k1}(\lambda) + \right.$$

$$\left. + \sin(k\varphi) \sum_{n=0}^{N-1} j_m(\tilde\lambda_n r) \int_{\lambda_n}^{\lambda_{n+1}} dz_m^{k2}(\lambda) \right], \quad \tilde\lambda_n = \lambda_n + \Delta/2, \tag{6}$$

and put $\eta_{A,N}(v) = \eta_{A,N,\infty}(v)$.

We show how to find such N for which

$$\Phi = \mathbf{E}|\eta_A(v) - \eta_{A,N}(v)|^2 < \varepsilon/3. \tag{7}$$

We have

$$\Phi = \sum_{m=0}^{\infty} \sum_{k=0}^{m} (A_m^k P_m^k(\cos\theta))^2 \sum_{n=0}^{N-1} \int_{\lambda_n}^{\lambda_{n+1}} |j_m(\lambda r) - j_m(\tilde\lambda_n r)|^2 f(\lambda)d\lambda.$$

It is possible to show that $\Phi < 4/3\, r_{max}^2\, \Delta^2$, where r_{max} denotes the maximal distance from the origin to the point in which the fields is simulated. Therefore for $\Delta = \sqrt{\varepsilon}/(2r_{max})$ and $N = A/\Delta$ inequality (7) is fulfilled.

Let us show now how to choose value M for which the inequality

$$\Psi = \mathbf{E}|\eta_{A,N}(v) - \eta_{A,N,M}(v)|^2 < \varepsilon/3 \tag{8}$$

is fulfilled. It is simple to verify that

$$\Psi = \sum_{m=M}^{\infty} (2m+1) \sum_{n=0}^{N-1} |j_m(\tilde\lambda_n r)|^2 \int_{\lambda_n}^{\lambda_{n+1}} f(\lambda)d\lambda.$$

If value M is such that $eAr_{max}/(2M+1) < 1$ then it is possible to verify that

$$\Psi < \frac{1}{2Ar_{max}} \left(\frac{eAr_{max}}{2M+1} \right)^{2M+1} \frac{1}{1 - \left(\dfrac{eAr_{max}}{2M+1} \right)^2}.$$

By equating the right side of the last inequality to value $\varepsilon/3$, we find value M for which inequality (8) is valid.

Hence from inequalities (5), (7), and (8) it follows that $\mathbf{E}|\eta(v) - \eta_{A,N,M}(v)|^2 < \varepsilon$.

In relation (6) the stochastic integrals $\int_{\lambda_n}^{\lambda_{n+1}} dz_m^{ks}(\lambda)$ may be changed by the values $\sqrt{\int_{\lambda_n}^{\lambda_{n+1}} f(\lambda)d\lambda}\, \xi_{mn}^{ks}$, where the random values ξ_{mn}^{ks} with the zero means and the unit variances are orthogonal with respect to parameter n and they are independent with respect to the rest parameters.

Under some restrictions on $f(\lambda)$ it is possible to change $\sqrt{\int_{\lambda_n}^{\lambda_{n+1}} f(\lambda)d\lambda}$ by $\sqrt{f(\tilde{\lambda}_n)\Delta}$. The expectation of the square difference Θ between these approximations does not exceed the value

$$\Theta \leq \sum_{n=0}^{N-1} \left| \sqrt{\int_{\lambda_n}^{\lambda_{n+1}} f(\lambda)d\lambda} - \sqrt{f(\tilde{\lambda}_n)\Delta} \right|^2.$$

Therefore for the field $\eta(v)$ modeling the following relation is used

$$\tilde{\eta}(v) = \tilde{\eta}(r,\varphi,\theta) = \sqrt{\Delta} \sum_{m=0}^{M} \sum_{k=0}^{m} A_m^k P_m^k(\cos\theta) \times$$

$$\sum_{n=0}^{N-1} j_m(\tilde{\lambda}_n r)\sqrt{f(\tilde{\lambda}_n)} \times \left[\cos(k\varphi)\xi_{mn}^{k1} + \sin(k\varphi)\xi_{mn}^{k2} \right]. \tag{9}$$

If the random values ξ_{mn}^{ks} are independent, and they have a stable distribution, then the field $\eta(v)$ has the same distribution. In partial for the Gaussian field $\eta(v)$ all processes $z(\lambda)$ in relation (1) and also values ξ_{mn}^{ks} are to be Gaussian.

By affinity of the obtained field it is possible to get some kinds of the homogeneous non-isotropic field [2].

As an examples the field simulation on the surfaces of the ellipsoid and of the cylinder.

References

[1] Yadrenko M.I.(1980) *The Spectral Theory of Random Fields.* Kiev. [Russian]

[2] Tovstik T.M., Vinogradova I.A., Myshenskaya V.A.(2001) On the Simulation of the Gaussian Random Field on the Ellipsoid and Cylinder Surface. *Proc. 4th St. Petersburg Workshop on Simulation.* pp. 476-480.

Prasana K. Venkatesh [1]
Schlumberger-Doll Research
Ridgefield, CT 06877, USA.
e-mail: `prasana@slb.com`

Title

Stochastic Lagrangian Models of Turbulent Flow - a Comparison of the Path-Integration, Quasi-Monte Carlo, and Monte Carlo Approaches

Abstract

In analogy with the Feynman-Kac path integration formulation of quantum mechanics, a general path integration formulation of stochastic-Lagrangian models of turbulent flow is developed with respect to the equivalence with the usual Eulerian and stochastic-Lagrangian descriptions. We then discuss efficient numerical methods for the realisation of the Lagrangian path integration which provide an effective alternative to the simpler Monte-Carlo approach. The dynamical variables in the aforesaid models are velocity, the dissipation rate, and passive or reactive scalars. The presentation will concern itself with path integrals in the configuration or phase space and also with the manner of efficiently representing and computing the analogues of quantum mechanical propagators of the Schroedinger and Fokker-Planck equations. The development is sufficiently general to also allow restricted Markovian evolution of fluid elements, e.g., those requiring forcing by non-standard Brownian dynamics, which is necessary in a Lagrangian description of intermittency in turbulent flows. Computational comparisons of the path-integration, quasi-Monte Carlo, and Monte-Carlo approaches to the simulation of particle-paths for a fully inhomogeneous turbulent flow problem will also be given.

Karin Schaber

SHYM Technology
75 Second Avenue
Needham
MA 02494, USA
e-mail: `Karin.Schaber@gmx.at`

Stefan Wegenkittl

SRS Medizintechnik
TechnoZ V, 2nd floor
Jakob Haringerstr. 8
A-5020 Salzburg, Austria
e-mail: `Stefan.Wegenkittl@ism-austria.at`

Title

Conditional Entropy Measures for Pseudorandom Numbers [1]

Abstract

In our presentation, we borrow the notion of unconditional secureness from the field of cryptoanalysis. Formulated in terms of conditional entropy and mutual information, this concept enables us to use some of the powerful methods developed in pseudorandom number (PRN) analysis.

Continuous measures like Discrepancy, Diaphony, and Spectral Test are mostly used in theoretical analysis employing the techniques of Weyl sums and spectral analysis. Black-box tests from the family of discrete Goodness-Of-Fit statistics (e.g. serial tests) on the other hand play a dominant role in the empirical quality assessment. Here, relative frequency is the key concept used to estimate probabilities.

Recently, a series of articles considered figures of merit based on entropy. Entropy can either be estimated from relative frequencies, or by return time analysis. A certain subfamily of serial tests was shown to be equal to a properly scaled version of entropy estimates.

For our test based on mutual information and conditional entropy we formulate both: an empirical test built on relative frequency and a version in terms of Walsh transforms more suited to theoretical analysis. We also give a sample application to the Hammersley point set. The test may be interpreted as the average behaviour of pairs of random numbers from subsequences with different lags.

Key Words

uniform distribution, pseudorandom numbers, entropy and information, Walsh transform

---

Ikumasa Yoshida [1]
Tadanobu Sato
Geotechnical and Structural Engineering Dept.
Tokyo Electric Power Services Co.,Ltd.
3-3-3, Higashi-Ueno Taito-ku, Tokyo, Japan
e-mail: `dyoshida@tepsco.co.jp`

TITLE

Non-Gaussian Nonlinear Damage Detection by Monte Carlo Filter

ABSTRACT

Non-Gaussian nonlinear filtering methods are relatively new topics these days. Basically the non-Gaussian nonlinear filtering methods need lots of computation efforts. However, new kinds of approach with using Monte Calro technique are becoming practical tools, such as Genetic Algorithm, because of the remarkable progress of computer performance. Monte Carlo Filter(MCF) proposed by Kitagawa is one of the methods, which can deal with non-Gaussian noises, and the probability distributions are expressed by many particles, in other words, sampled realizations. The behavior of each particle is simulated and tracked by assumed model in MCF, while only first and second moments of the probability distributions are estimated in Kalman filter.

One of the application of these filtering methods in civil engineering is damage detection of structures. After a large earthquake, rapid damage estimation of structures, especially important structures such as hospitals, bridge, firehouses and so on, is needed to prevent the secondary disasters. However, huge time and cost are necessary to evaluate the damage of all the structures, if we inspect visually structural damage in detail, which is conventional way. A practical method for rapid damage detection of the structures with the monitored data is desirable from the standpoint of damage detection or health monitoring. Linear/Nonlinear identification methodology has been studied, and various methods are proposed by many researchers. Kalman filter is the most famous and widely used in many fields due to its beautiful and simple algorithm which needs only first and second moment of the probabilistic nature, because Kalman filter is well established based on linear Gaussian assumptions. Though many types of nonlinear identification methods are studied and proposed, but most of them have the same limitation as Kalman filter has, because most of the proposed methods are based on Gaussian noises which leads to quadratic form objective function (cost function) . In other words, L2 norm is used in order to make the objective function. When the nature of damaged structure is considered, other type of noises might be preferable. The minor damage due to earthquake tends to be localized, in other words, the damage concentrates in limited parts. Of course, when the destructive huge earthquake hits, damages will occur in many parts at the same time. However, we do not need cautious inspections for the structure with the major damage, because it is clear that the structure is severely damaged. In the purpose

---

[1]Speaker

of damage detection, the minor to moderate damages are important. In order to detect this minor to moderate damage, Gaussian process noise (L2-norm) may not be proper.

In this paper, the method of damage detection using the Monte Calro filter is proposed and demonstrated. First, the formulation of the identification using Monte Calro filter is presented, which is natural extension of Kalman filter (linear Gaussian), but essential difference is that we need not to use the Gaussian noises. Through numerical simulations of damage detection by MCF with Gaussian or non-Gaussian process noise, the importance of the type of process noises is demonstrated. In this numerical example, hypothetical 5-DOF model is used. It is assumed that the damage occurs at specific one element, where the stiffness decreases from 400 to 360 tf/m^2, and damping ratio increases from 0.02 to 0.04 during earthquake. Due to this damage, the fundamental frequency of the model is reduced from 1.0Hz to 0.99Hz. The observation data used for the damage detection are simulated structural responses adding 3% (rms ratio) Gaussian white noises. The number of particles is 1000. The identification with up to particle number 10000 is tried, but the performance is almost same, while in the case of less than 1000, the performance becomes worse. For the case of SDOF system, good results are obtained even if the particle number is 100.

The distributions of particles of the estimated stiffness and damping ratio give directly the non-stationary probability density function of the identified parameters. When observation data at all nodes is used, the peak of estimated stiffness distribution is clearly detected. While we use observations at node 1 and 3, the peak of distribution becomes vague, but still we can observe the change of structural parameters. We can also observe the change of the damping ratio, but generally it is not clear. Though the many simulations are conducted under various conditions, to identify change of damping ratio is very difficult. Since identification of damping ratios are very unstable, we use only the change of stiffness to identify the damage of structures. When the observation data of all nodes are used, the damage is detected properly despite of types of process noise. While the observed data is limited to node 1 and 3, the case with non-Gaussian process noise seems to be better than the case with Gaussian process noise in this numerical simulation. These results suggest us that MCF with non-Gaussian process noise is suitable for the damage detection.

In MCF, the identified parameters sometimes vary depending on the numerical conditions such as particles number, seed of random number and parameters for the noise. Further improvements such as adaptive tuning, proper type of process noise, more stable algorithm are needed to develop a practical tool. However, MCF seems to be very prospective for the damage detection of a structure, because it can be applied to a broad class of non-linear and non-Gaussian problems.

Sergey K. Kochuguev [1]
Victor V. Kunitsyn
Dmitry Kh. Ofengeim [1]
SoftImpact Ltd.
194156 P.O.Box 33
St.Petersburg, Russia
e-mail: `sergey@softimpact.fi.ru`
e-mail: `dima@softimpact.fi.ru`

Alexander I. Zhmakin [1]
A.F.Ioffe Physical Technical Institute
Russian Academy of Sciences
194021 St.Petersburg, Russia
e-mail: `zhmakin@softimpact.fi.ru`

Title

Optimization of a Ray Tracing Method for Radiative Heat Transfer Problems

Abstract

Numerical study of the industrial growth of crystals is an important factor of the progress in this field since experimental approach is extremely expensive in terms of both time and money. Final goals of the simulation are optimization of the growth processes and design of the growth facilities.

A simulation of the crystal growth requires solution of a number of sub-problems in the complex geometry of the real-life growth equipment (1). Usually one has to compute fluid flow and mass transfer in the reactor channel (2) coupled to the global heat transfer in gas and in all solid parts of the growth reactor. Due to the high temperatures of the process radiative heat transfer is, as a rule, a dominant mechanism. Depending on the growth process in question, the complexity of the radiative heat transfer model can vary from a relatively simple one such as grey radiation via view factors ("surface-to-surface") (3) to rather elaborate multi-band models that account for both diffuse and specular reflections from boundaries and for the presence of semi-transparent bodies.

Monte Carlo method is a powerful and flexible tool to simulate radiative heat transfer in complex geometry that takes into account all the relevant optical phenomena (absorption, scattering, refraction, diffuse and specular reflection) (4; 5).

An efficient method based on this approach – The Ray Tracing Method – has been proposed in (6) for a 3D computations. It generalizes a view factors concept to the general case (view factors for the arbitrary - diffuse or specular - surface and semi-transparent volume elements). Monte Carlo process is used to compute diffuse and absorbtion view factors by tracking the history of rays (representing bundles of radiative energy) that are emitted by both surface and volume elements.

However, the Ray Emission Model described in (6) fails to account for semi-transparent media with a large absorption coefficient, which, in turn, does not allow one to apply the method for multiband computations. In (7; 8) a modified Ray Emission Model has been proposed to

---

make this method applicable to multiband computations and radiation transfer simulations in media with large absorption coefficients. The method described in (6) has been also modified for efficient computations in an axisymmetrical case.

This paper discusses further improvements of the Ray Tracing Method. The numerical approach of the Ray Emission Model have been analyzed and improved. Specific physical effects, such as ray interference in thin semi-transparent layers have been taken into account.

The Modified Ray Tracing Method has a common drawback of Monte Carlo methods: an unfavorable trade-off between computation time and prediction accuracy (9). In the present paper a number of approaches to optimized computational procedure has been studied including universal ones such as pencil tracing technique, search acceleration routines etc. as well as specialized techiques that are applicable to the restricted classes of problems only but provide drastic reduction of the execution time.

The Modified Ray Tracing Method will be illustrated by both test problems and computations in the real-life growth equipment. The first example is the heat transfer in the reactor chamber used for growth of silicon carbide by sublimation method where the gray radiation model provides sufficient accuracy. The three-band radiation model has been exploited for computation of the heat transfer in the large scale industrial epitaxial Centura Reactor where heating of a graphite susceptor provided by the radiation from halogen lamps surrounded by golden reflectors. The need to consider more complex model in this case results from the wavelegth dependence of the optical properties of quartz form which the reactor walls are made. The computations have shown, in particularity, that reactor walls are heated mainly not by the lamp radiation but by the secondary radiation from the substrate with much lower surface temperature.

References

[1] M.Meyyappan, Ed., *Computational Modeling in Semiconductor Processing*, The Artech House, 1995, 363 pp.

[2] Yu.E. Egorov, A.I. Zhmakin, *Numerical simulation of low-Mach number gas mixture flows with heat and mass transfer using unstructured grid*, Computational Materials Science, 11 (1998), pp. 204–220.

[3] F.Dupret, P.Nicodeme, Y.Ryckmans, P.Wouters, M.J.Crochet, *Global modeling of heat transfer in crystal growth furnaces* , Int. J. Heat Mass Transfer, 33 (1990) pp. 1849–1871.

[4] J.R.Howell, M.Perlmutter, *Monte Carlo solution of thermal transfer through radiant media between gray walls*, J. Heat Transfer 86 (1964) 116–122.

[5] A.Kersch, W.J.Morokoff, *Transport Simulation in Microelectronics*, Birkhäuser Verlag, Basel–Boston–Berlin, 1995.

[6] S.Maruyama, T. Aihira, *Radiation heat transfer of arbitrary three-dimensional absorbing,emitting and scattering media and specular and diffuse surfaces* , J. Heat Transfer, 119 (1997) pp. 129–136.

[7] S.Kochuguev, D.Ofengeim, A.Zhmakin, *Axisymmetrical radiative heat transfer simulation by Ray Tracing Method*, Proceedings of the 3rd European Conference on Numerical Mathematics and Advanced Applications, P. Neittaanmäki, T. Tiihonen and P. Tarvainen (eds.), World Scientific, Singapore, 2000, pp. 579-586.

[8] S.Kochuguev, D.Ofengeim, A.Zhmakin, A.Galyukov, *Adaptive multigrid methods for crystal growth problems on unstructured/hybrid grids*, Proceedings of the 16th IMACS World Congress, Lausanne, August 2000.

[9] M.Kobiyama, *A study on the reduction of computing time of the Monte Carlo method applied to the radiative heat transfer*, Bulletin of JSME 29 (1986) 3000–3006.

List of Participants